MR No. E6E27

NATIONAL ADVISORY COMMITTEE FOR AERONAUTICS

WARTIME REPORT

ORIGINALLY ISSUED

June 1946 as
Memorandum Report E6E27

AERODYNAMICS OF THE CARBURETOR AIR SCOOP AND THE ENGINE COWLING OF A SINGLE-ENGINE TORPEDO-BOMBER-TYPE AIRPLANE

By John K. Kuenzig and Herman Palter

Aircraft Engine Research Laboratory
Cleveland, Ohio

NACA

WASHINGTON

NACA MR No. E6E27

NACA AIRCRAFT ENGINE RESEARCH LABORATORY

MEMORANDUM REPORT

for the

Bureau of Aeronautics, Navy Department

AERODYNAMICS OF THE CARBURETOR AIR SCOOP AND THE ENGINE COWLING OF A SINGLE-ENGINE TORPEDO-BOMBER-TYPE AIRPLANE

By John K. Kuenzig and Herman Palter

SUMMARY

An investigation was conducted in the NACA Cleveland altitude wind tunnel on the carburetor air scoop and the engine cowling of a single-engine torpedo-bomber-type airplane. Low pressure recoveries were obtained at the carburetor top deck as a result of inadequate removal of the boundary-layer air ahead of the inlet. Investigation of the engine cowling showed low pressure recoveries at the face of the engine, which were attributed to propeller interference. These low pressure recoveries were further decreased at high angles of attack by the blocking effect of the spinner. Pressure losses of the carburetor-scoop duct and the cowl diffuser were each roughly 10 percent of the dynamic pressure.

INTRODUCTION

An investigation of the power-plant installation of a single-engine torpedo-bomber-type airplane has been conducted in the NACA Cleveland altitude wind tunnel at the request of the Bureau of Aeronautics, Navy Department. As a part of this investigation, the aerodynamic characteristics of the carburetor air scoop and the engine cowling were determined. A similar investigation was previously conducted on a three-tenths scale mock-up of the forward portion of the fuselage of this airplane in the Langley 20-foot tunnel. (See reference 1.)

The aerodynamic characteristics of the carburetor air scoop are of particular interest because of the use of a boundary-layer

removal duct with the scoop, which is located behind and above the engine cowling. Both internal and external flow conditions were investigated.

The effectiveness of the engine cowling, a high inlet velocity type, was evaluated on the basis of internal and external flow conditions. The flow conditions were varied over a wide range by changing both the tunnel airspeed and the engine cowl-flap position.

DESCRIPTION OF MODEL

Tests were made with a full-scale model of the XTB2D-1 airplane with the empennage removed and the wing tips cut to permit mounting in the 20-foot-diameter test section of the tunnel. (See fig. 1.) The power plant of the model is a 28-cylinder, air-cooled, radial engine with a normal rated power of 2500 brake horsepower at an engine speed of 2550 rpm and a take-off power of 3000 brake horsepower at 2700 rpm. The engine power is absorbed by a counter-rotating propeller, which rotates at 0.425 engine-crankshaft speed. This propeller is 14 feet in diameter and consists of two components of four blades each.

Carburetor Air Scoop

The carburetor air scoop is located behind and above the engine cowling. (See figs. 2 and 3.) The small adjacent duct opening is the cabin-heater air inlet. The air from this duct was discharged into the engine accessory compartment during the tests. A boundary-layer removal duct is located beneath each entrance. The cross-sectional area of the carburetor air duct is approximately 74 square inches. The effective carburetor top-deck area was reduced from 100 to 75 square inches by means of a duct fairing (fig. 2).

Engine Cowling

The cowling inlet is formed by a nose ring with a minimum inside diameter of 37.75 inches and a spinner with a diameter of 25.88 inches; the minimum entrance area is 480 square inches. Control of the exit area is accomplished by 11-inch chord flaps, which extend approximately 220° around the circumference of the cowling. A calibration of cowl-flap deflection against cowl-flap gap and exit area is given in figure 4.

INSTRUMENTATION

Instrumentation was installed for taking total-pressure surveys ahead of the scoop entrance, at the scoop, and at the carburetor top deck, and for taking a static-pressure survey over the scoop lip. (See fig. 3.) Total-pressure surveys of the cowling included surveys of the cowling inlet, the face of the engine, and the cowling exit. Static-pressure orifices were installed over the upper and lower cowling lips. The static pressure at the rear of the engine was measured by tubes located on the baffles of the rear-row cylinders of the engine.

The drag was determined from force readings taken with the tunnel balance.

SCOPE OF TESTS

Carburetor-scoop tests were made in which the inclination of the thrust axis of the model was varied from -2° to 6° and the inlet-velocity ratio from 0.2 to 0.8. These tests were conducted at a pressure altitude of 5000 feet.

Tests to evaluate cowling performance were made with the propeller operating and with the propeller removed. The propeller-operating tests were made at varying engine powers, cowl-flap deflections, and tunnel airspeeds at an inclination of the thrust axis of 0°. Pressure altitudes ranged from 5000 to 30,000 feet. The tests with the propeller removed were conducted at a pressure altitude of 15,000 feet, inclinations of the thrust axis of 0° to 6°, and varying cowl-flap deflections.

SYMBOLS

For convenience, all symbols used in this paper, the table, or the figures are listed here in alphabetical order.

ΔD incremental drag, drag of installation for condition under consideration minus lowest drag for a series of tests in which only the cowl-flap deflection was changed, pounds

$\frac{\Delta D}{q_o}$ incremental-drag coefficient

H total pressure, pounds per square foot

$\frac{H - p_o}{q_c}$ total-pressure coefficient

ΔH incremental total pressure, pounds per square foot

$\frac{\Delta H}{q_c}$ carburetor duct losses

p static pressure, pounds per square foot

$\frac{p - p_o}{q_c}$ static-pressure coefficient

p_c free-stream static pressure, pounds per square foot

Δp cooling-air pressure drop across engine, total pressure at front minus static pressure at rear, inches of water

$\frac{\Delta p}{q_c}$ pressure-drop coefficient

$\sigma \Delta p$ cooling-air pressure drop, inches of water

q_c free-stream impact pressure shown by pitot-static tube, pounds per square foot

q_c free-stream dynamic pressure, pounds per square foot

ρ mass density, slugs per cubic foot

σ density ratio, $\rho/0.002378$

RESULTS AND DISCUSSION

Carburetor Air Scoop

External flow. - The total-pressure losses ahead of the air scoop were a combination of the losses resulting from propeller interference and the losses caused by boundary-layer formation. These losses in energy of the air were determined by total-pressure surveys taken with two pressure rakes located ahead of the scoop inlet (fig. 3). These total pressures are shown in figure 5 as constant-pressure contours and are not to be misconstrued as stream

lines. The effect of the propeller on these pressure contours cannot be isolated because of insufficient data. An increase in the inlet-velocity ratio of the scoop decreases the boundary-layer thickness as evidenced by figures 5(a) and 5(b). An increase in the inclination of the thrust axis, however, increases the boundary-layer thickness as shown by figures 5(c) and 5(d). This increase in boundary layer causes low total-pressure recoveries at the scoop inlet and indicates that the boundary-layer removal duct had insufficient capacity to remove the boundary layer.

The static-pressure survey over the carburetor-scoop lip is given in figure 6 for conditions corresponding to those of figure 5. The negative pressure peaks are only slightly affected by variations in inlet-velocity ratio or angle of attack. No critical velocities over the scoop lip would be expected within the speed range of the airplane. The static-pressure coefficient $\frac{p - p_o}{q_o}$, which is plotted in figure 6, is based on the static and dynamic pressures ahead of the model.

Internal flow. - Examination of the pressure distribution of the air entering the scoop inlet revealed that high pressures were obtained at the side nearest the cabin-heater duct, as shown in figure 7. The high pressures were attributed to the removal of part of the boundary-layer air ahead of the scoop by the cabin-heater duct.

The effect of free-stream impact pressure on total-pressure recovery at the carburetor top deck for various inlet-velocity ratios and inclinations of the thrust axis is given in figure 8. The high recoveries at low free-stream impact pressures and low recoveries at high free-stream impact pressures indicate that the blade angle at the propeller-blade roots was too low. The design of the pitch distribution of the propeller should be investigated further.

The high pressures on the right side of the air scoop were reflected on the carburetor top deck, as shown in figure 9. The carburetor-scoop duct losses were roughly 10 percent of the dynamic pressure, as shown in table I.

Engine Cowling

External flow. - The effect of inclination of the thrust axis on pressure distribution over the upper and lower lips of the engine cowling is given in figure 10. The pressure-distribution pattern

in this figure is typical of all conditions tested. Owing to the high inlet-velocity ratio of this cowling, the negative pressure peaks occur on the inner surface of the cowling lip. As the inclination of the thrust axis is increased, these pressure peaks increase on the lower lip and decrease on the upper lip. The maximum negative pressure peaks indicate that critical velocities over the lip surface would not be reached within the speed range of the airplane.

Internal flow. - The effect of cowl-flap deflection and free-stream impact pressure on total-pressure recovery at the cowling inlet for tests with the propeller operating and the propeller removed is shown in figure 11. This figure also shows a loss of pressure recovery of approximately $0.25/q_c$ owing to the blocking effect of the propeller. The low pressure recoveries are then reflected at the face of the engine (fig. 12) with an additional loss as the air passes through the cowling diffuser. The cowl-diffuser losses of approximately $0.1/q_c$ are shown in figure 13.

The average total pressures at the cowling inlet were only slightly influenced by changes in the inlet-velocity ratio for propeller operating tests. (See fig. 14.) Higher pressures were obtained with the propeller removed for the range of inlet-velocity ratios covered.

The effects of changes in the inclination of the thrust axis on the total-pressure distribution pattern of the cowling inlet for tests with the propeller operating and the propeller removed are shown in figures 15 and 16, respectively. The total-pressure distribution patterns were fairly symmetrical about the thrust axis for small angles of attack, whereas at large angles of attack a reduction in pressure recovery occurred in the upper half of the inlet. This reduction indicated that the boundary layer over the spinner was washed to the top of the spinner and entered the upper portion of the cowling. (See figs. 15(c) and 16 (c).)

The effect of free-stream impact pressure on the cooling-air pressure drop across the engine Δp for various cowl-flap deflections is shown in figure 17. For tests with the propeller removed and the propeller operating, the cooling-air pressure drop across the engine may be found for a given cowl-flap deflection and free-stream impact pressure. This pressure drop may then be converted to cooling-air flow by use of figure 18 for only cold engine conditions. No cooling-air flows for hot engine conditions could be obtained because of insufficient data.

Drag

The variation in incremental-drag coefficient $\Delta D/q_o$ with cowl-flap deflection for tests with the propeller removed is shown in figure 19. The incremental drag was derived by subtracting the lowest drag reading from all other drag readings. The variation of incremental-drag coefficient $\Delta D/q_o$ with $\Delta p/q_c$ across the engine for tests with the propeller removed is given in figure 20. No drag data for propeller-operating tests are included because insufficient readings were obtained.

SUMMARY OF RESULTS

The following results were obtained from an investigation in the Cleveland altitude tunnel of the carburetor air scoop and the engine cowling of a single-engine torpedo-bomber-type airplane:

1. The boundary-layer removal duct had insufficient capacity to remove the boundary layer ahead of the carburetor air scoop.

2. The carburetor-duct losses and the cowl-diffuser losses were roughly 10 percent of the dynamic pressure.

3. Low pressure recoveries at the face of the engine were caused chiefly by propeller interference.

4. The long spinner seriously blocked the air flow into the upper half of the cowling at high inclinations of the thrust axis.

Aircraft Engine Research Laboratory,
National Advisory Committee for Aeronautics,
Cleveland, Ohio.

REFERENCE

1. Nichols, Mark R., Keith, Arvid L., Jr., and Boswinkle, Robert W., Jr.: A Wind-Tunnel Investigation of Carburetor-Air Scoops Designed for the Douglas XTB2D-1 Airplane. NACA Memo. rep., Bur. Aero., June 7, 1944.

TABLE I. - LOSSES IN CARBURETOR-AIR-SCOOP DUCT

Charge-air weight flow (lb/hr)	Inclination of thrust axis (deg)	Air Scoop duct inlet-velocity ratio	Average total pressure coefficient $\frac{H-p_o}{q_c}$		Carburetor duct losses, $\frac{\Delta H}{q_c}$
			Carburetor scoop inlet	Carburetor top deck	
8,475	-2	0.533	1.60	1.56	0.04
8,437	6	.558	1.10	1.05	.05
10,990	-2	.512	1.25	1.12	.13
10,840	2	.508	1.01	.93	.03
10,720	6	.501	.83	.77	.06
12,540	-2	.492	.96	.87	.09
12,430	2	.492	.81	.74	.07
12,250	6	.496	.63	.58	.05
15,180	-2	.528	.94	.85	.09
15,170	2	.530	.78	.71	.07
16,580	2	.493	.71	.64	.07
16,480	6	.502	.54	.49	.05
13,210	2	.818	1.65	1.59	.06
15,990	2	.760	1.20	1.07	.13
16,110	6	.763	1.49	1.33	.16

National Advisory Committee
for Aeronautics

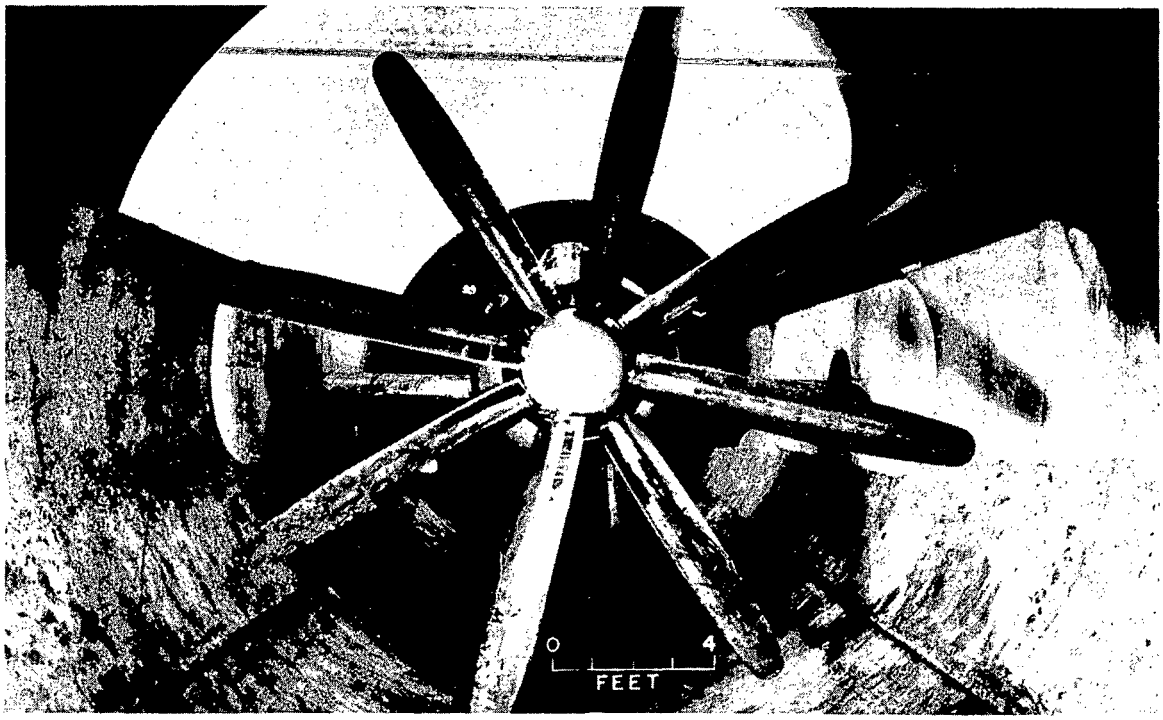

(a) Propeller installed.

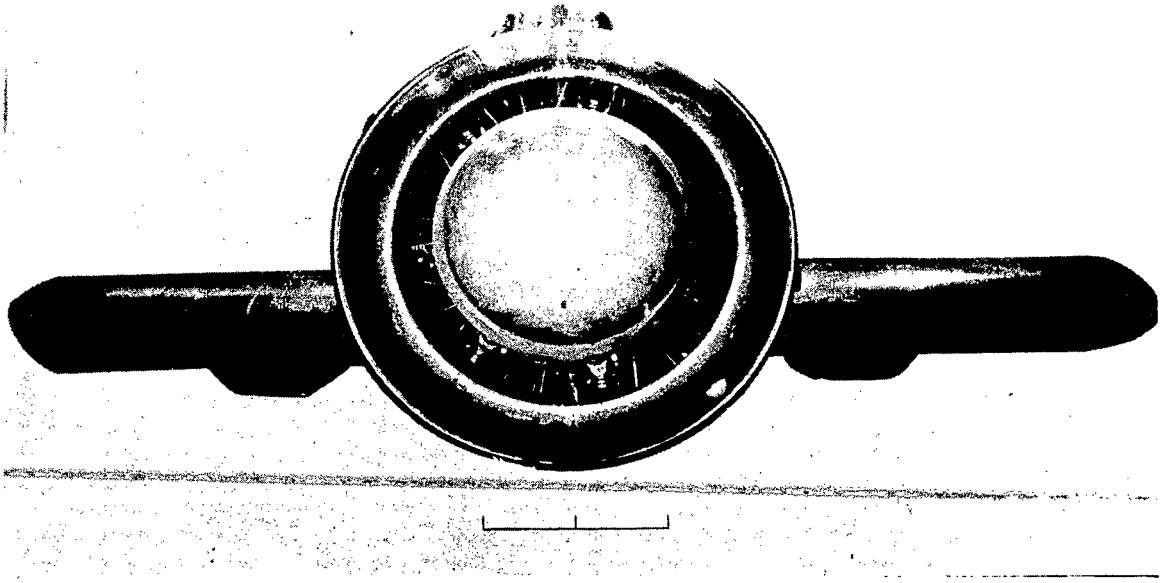

(b) Propeller removed.

Figure 1. - Full-scale model of single-engine torpedo-bomber-type airplane installed in altitude tunnel.

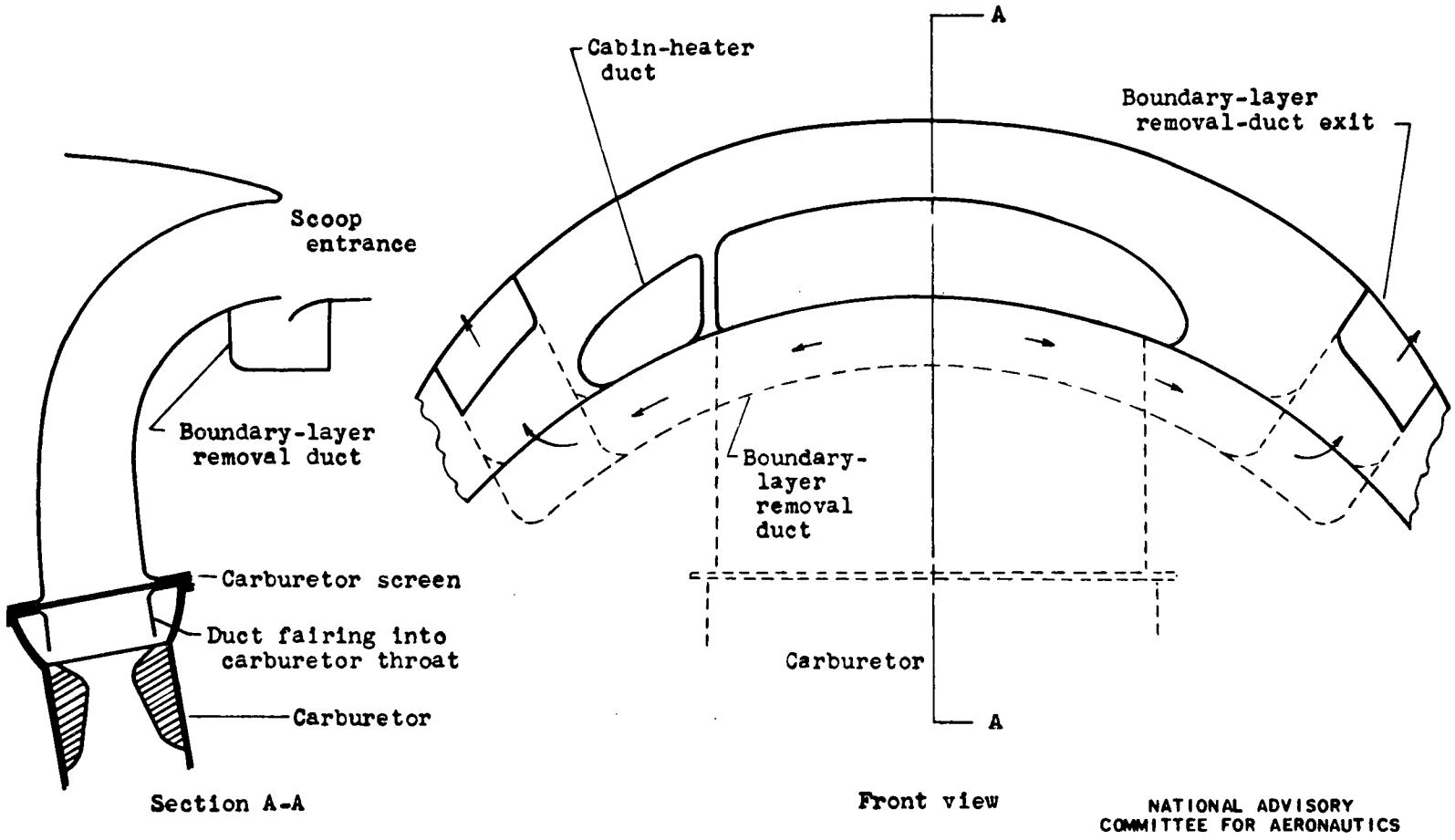

Figure 2. — Carburetor-air-scoop installation of single-engine torpedo-bomber-type airplane showing boundary-layer removel duct and duct fairing into carburetor.

NACA MR NO. E6E27

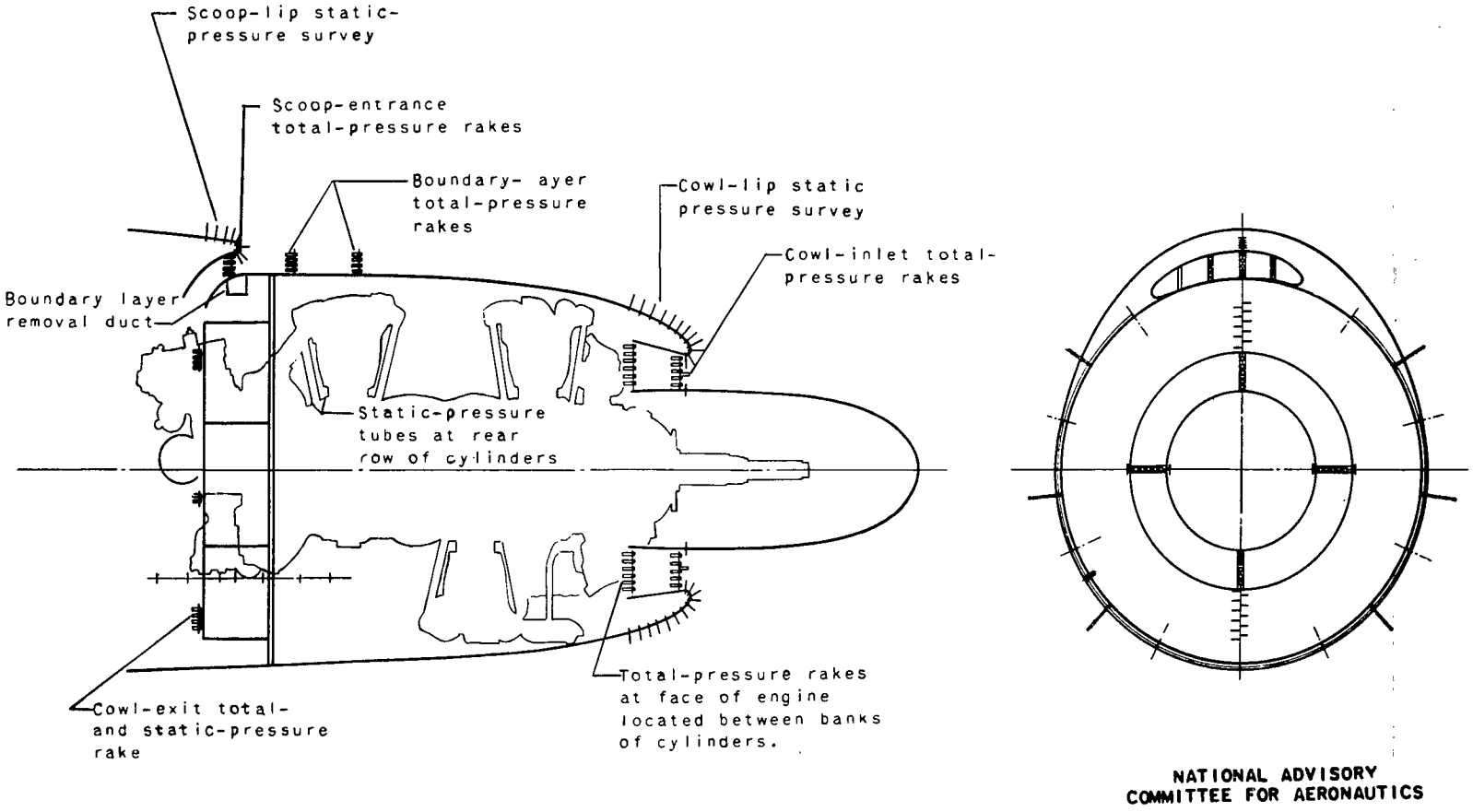

Figure 3. - Instrumentation for pressure survey of carburetor-duct inlet and engine cowling on single-engine torpedo-bomber-type airplane.

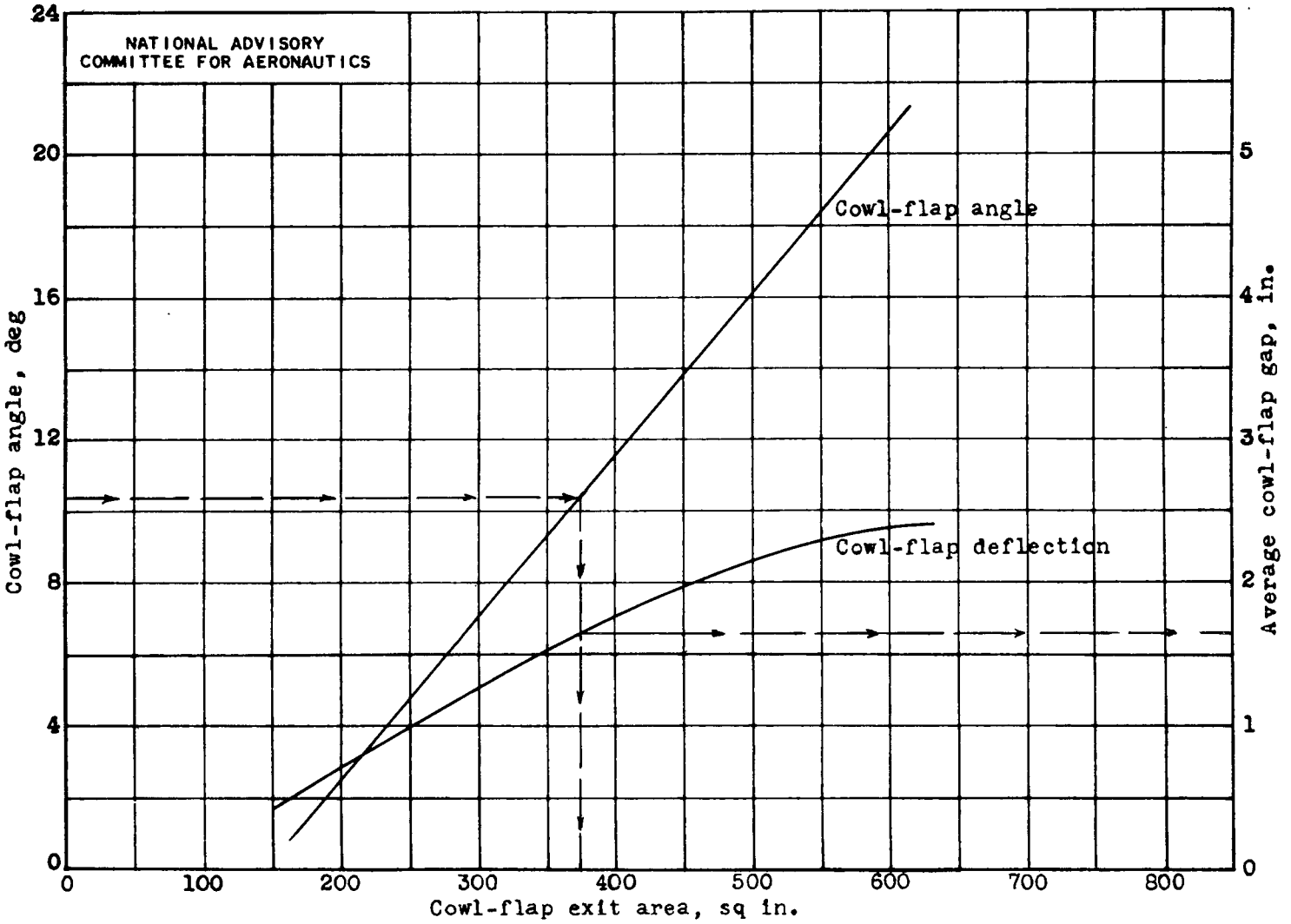

Figure 4. - Cowl-flap calibration for single-engine torpedo-bomber-type airplane with stub exhaust stacks installed.

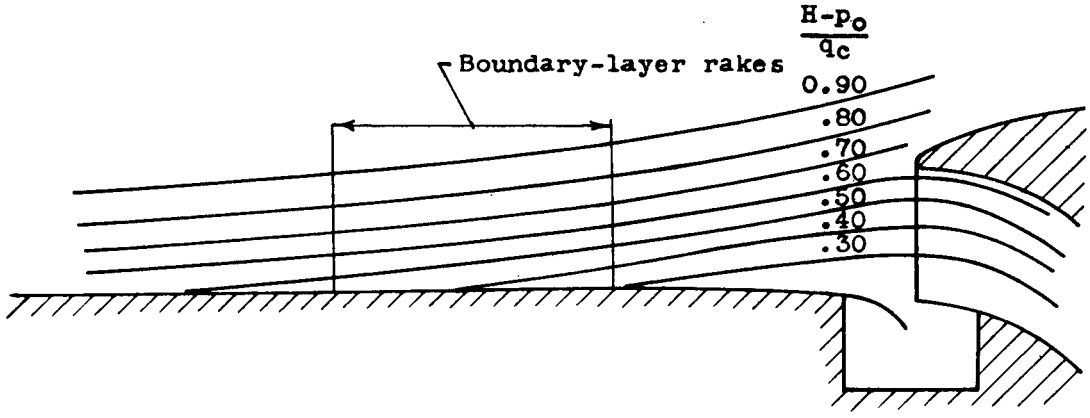

(a) Inclination of thrust axis, 2°; free-stream impact pressure, 43 pounds per square foot; inlet-velocity ratio, 0.2.

NATIONAL ADVISORY
COMMITTEE FOR AERONAUTICS

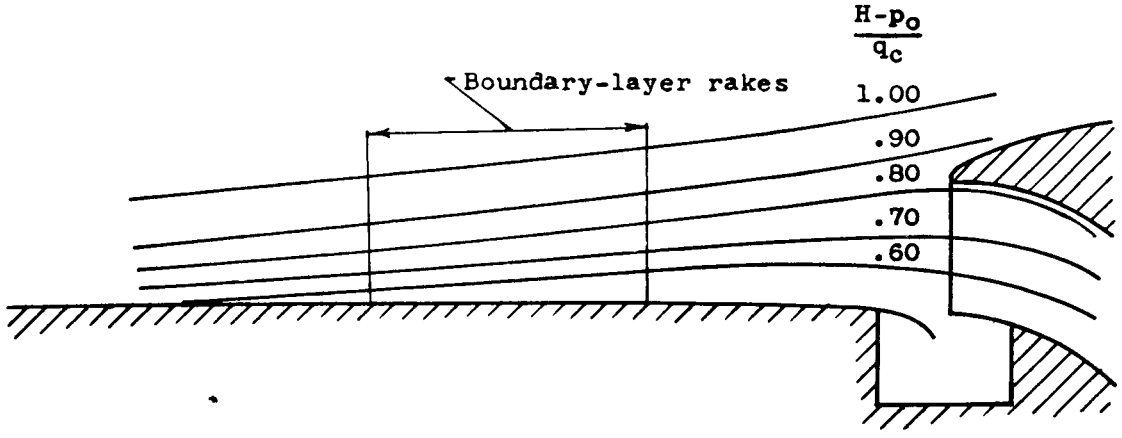

(b) Inclination of thrust axis, 2°; free-stream impact pressure, 46 pounds per square foot; inlet-velocity ratio, 0.5.

Figure 5. - Constant total-pressure-recovery contours of charge air entering carburetor air scoop of single-engine torpedo-bomber-type airplane. Pressure altitude, 5000 feet.

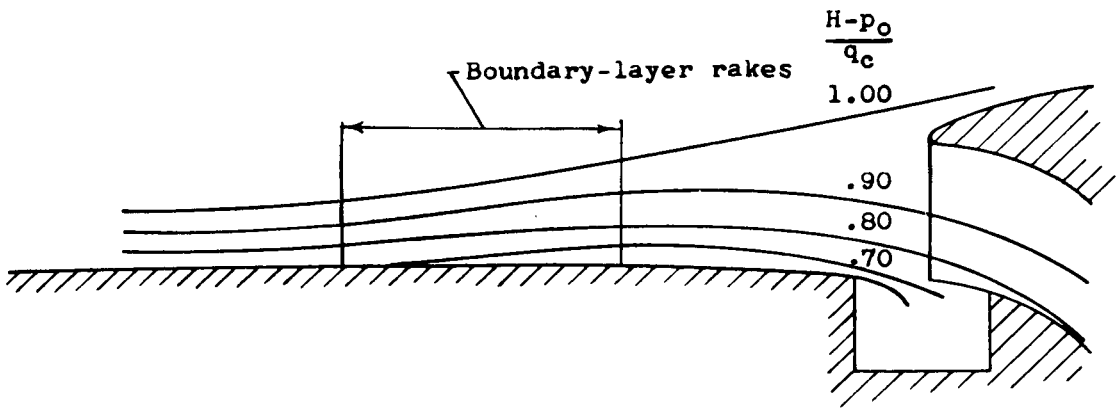

(c) Inclination of thrust axis, -2°; free-stream impact pressure, 46 pounds per square foot; inlet-velocity ratio, 0.5.

NATIONAL ADVISORY
COMMITTEE FOR AERONAUTICS

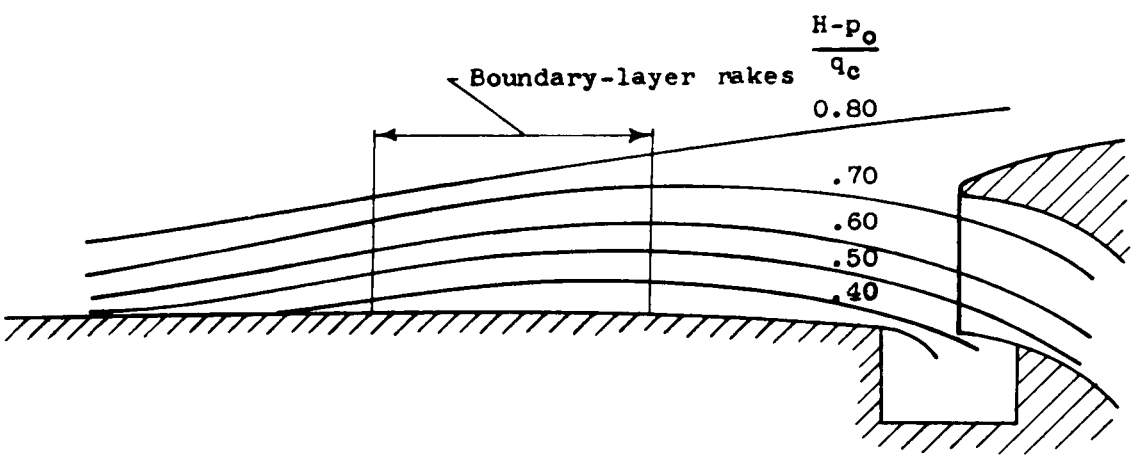

(d) Inclination of thrust axis, 6°; free-stream impact pressure, 46 pounds per square foot; inlet-velocity ratio, 0.5.

Figure 5. - Concluded. Constant total-pressure-recovery contours of charge air entering carburetor air scoop of single-engine torpedo-bomber-type airplane. Pressure altitude, 5000 feet.

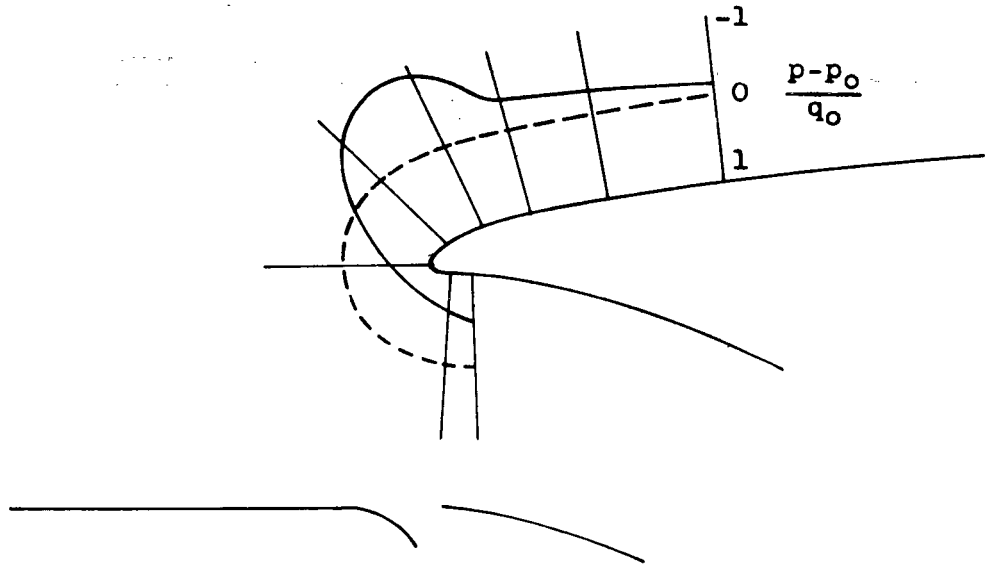

(a) Inclination of thrust axis, 2°; free-stream impact pressure, 43 pounds per square foot; inlet-velocity ratio, 0.2.

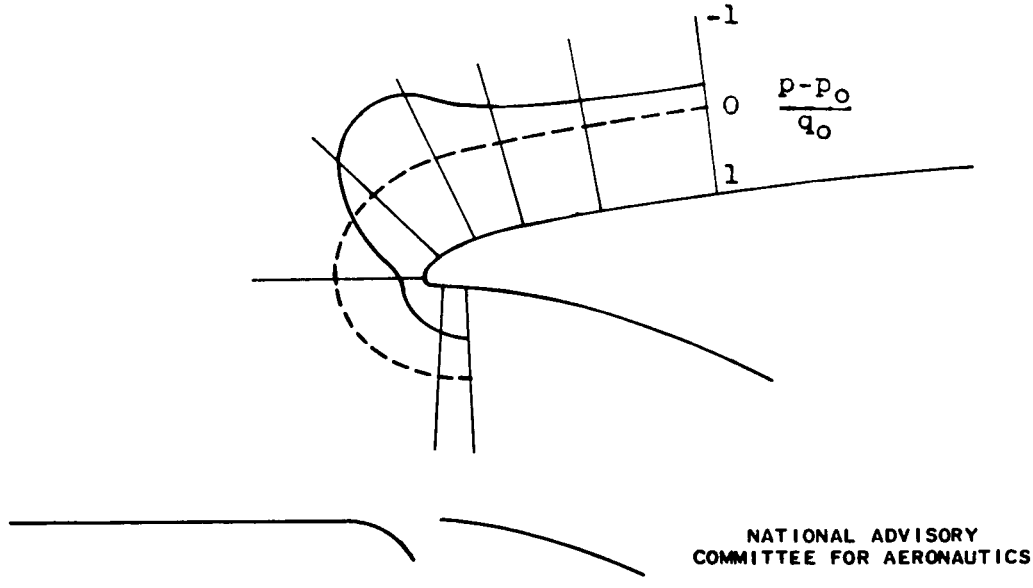

(b) Inclination of thrust axis, 2°; free-stream impact pressure, 46 pounds per square foot; inlet-velocity ratio, 0.5.

Figure 6. - Static-pressure survey of carburetor-scoop lip of single-engine torpedo-bomber-type airplane.

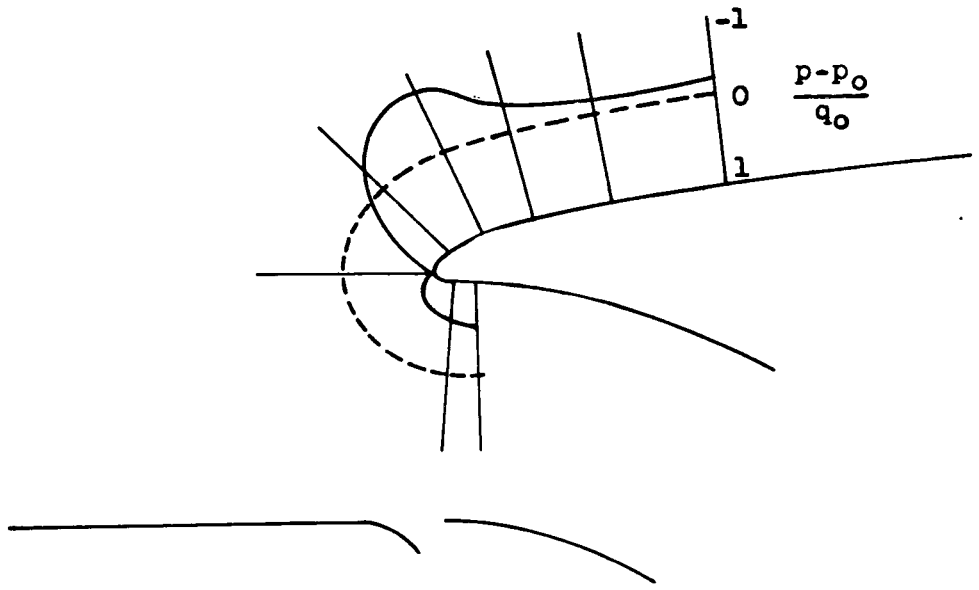

(c) Inclination of thrust axis, -2°; free-stream impact pressure, 46 pounds per square foot; inlet-velocity ratio, 0.5.

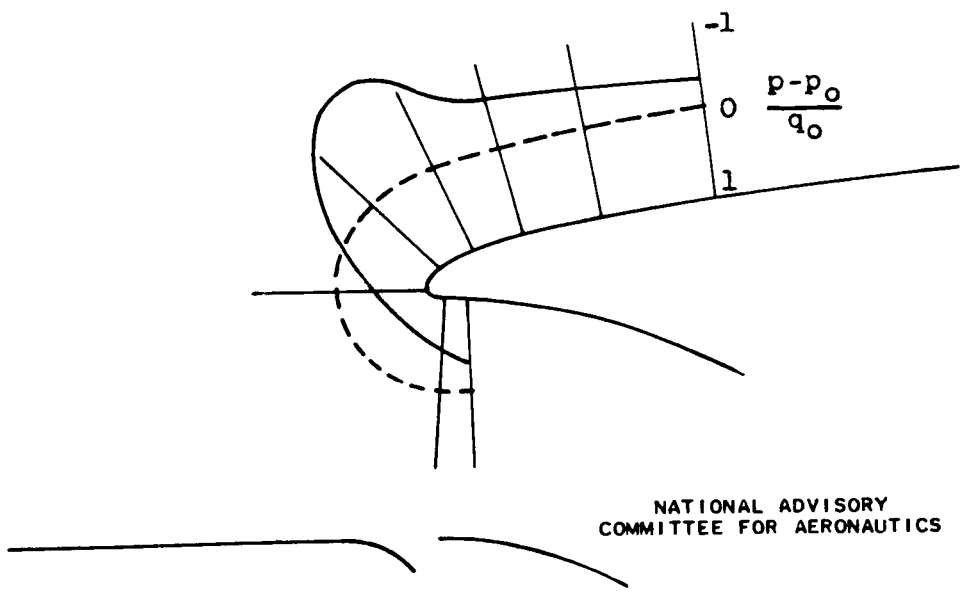

(d) Inclination of thrust axis, 6°; free-stream impact pressure, 46 pounds per square foot; inlet-velocity ratio, 0.5.

Figure 6. - Concluded. Static-pressure survey of carburetor-scoop lip of single-engine torpedo-bomber-type airplane.

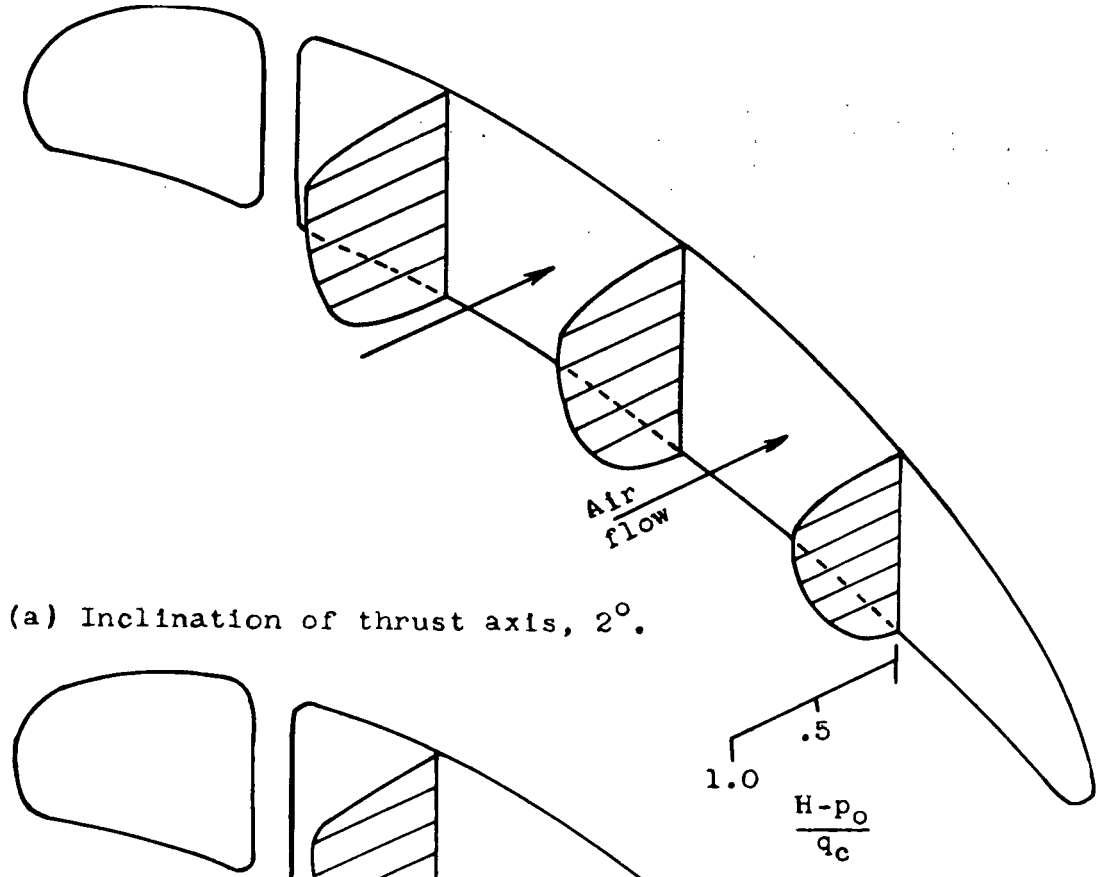

(a) Inclination of thrust axis, 2°.

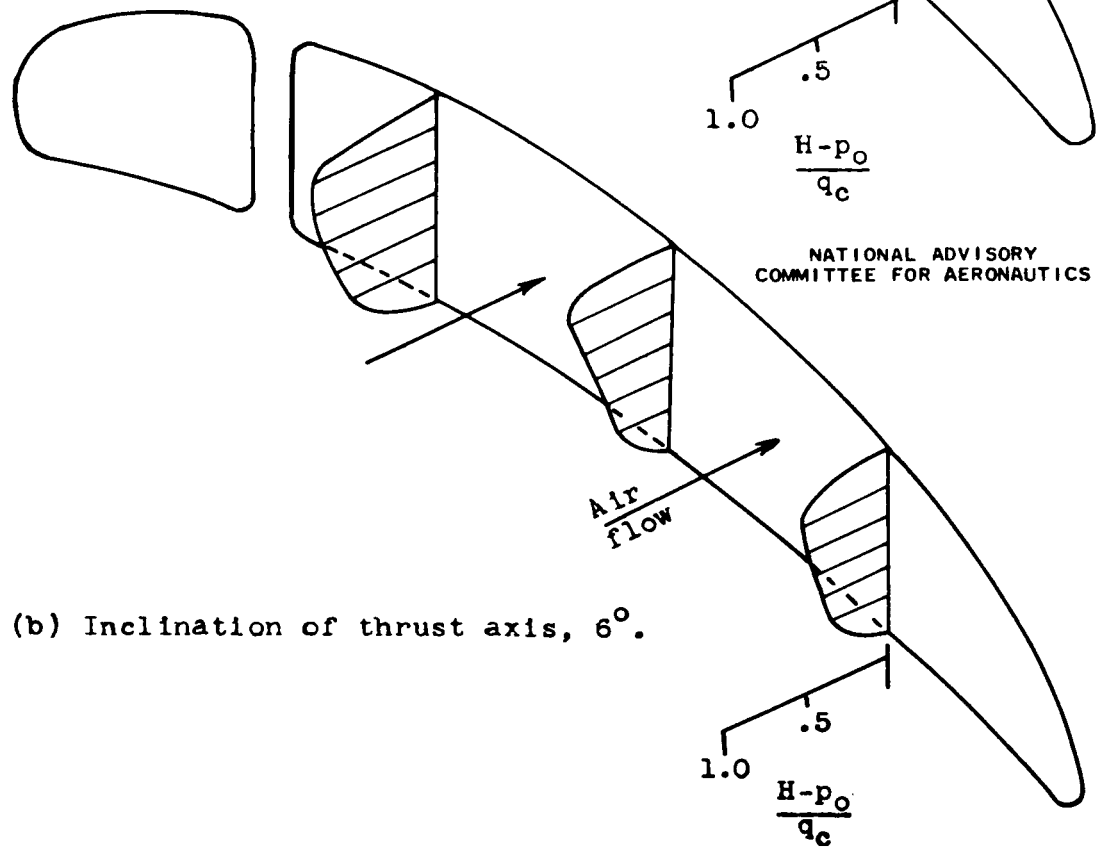

(b) Inclination of thrust axis, 6°.

Figure 7. - Typical pressure recovery at carburetor airscoop entrance of single-engine torpedo-bomber-type airplane. Propeller advance-diameter ratio, 0.337.

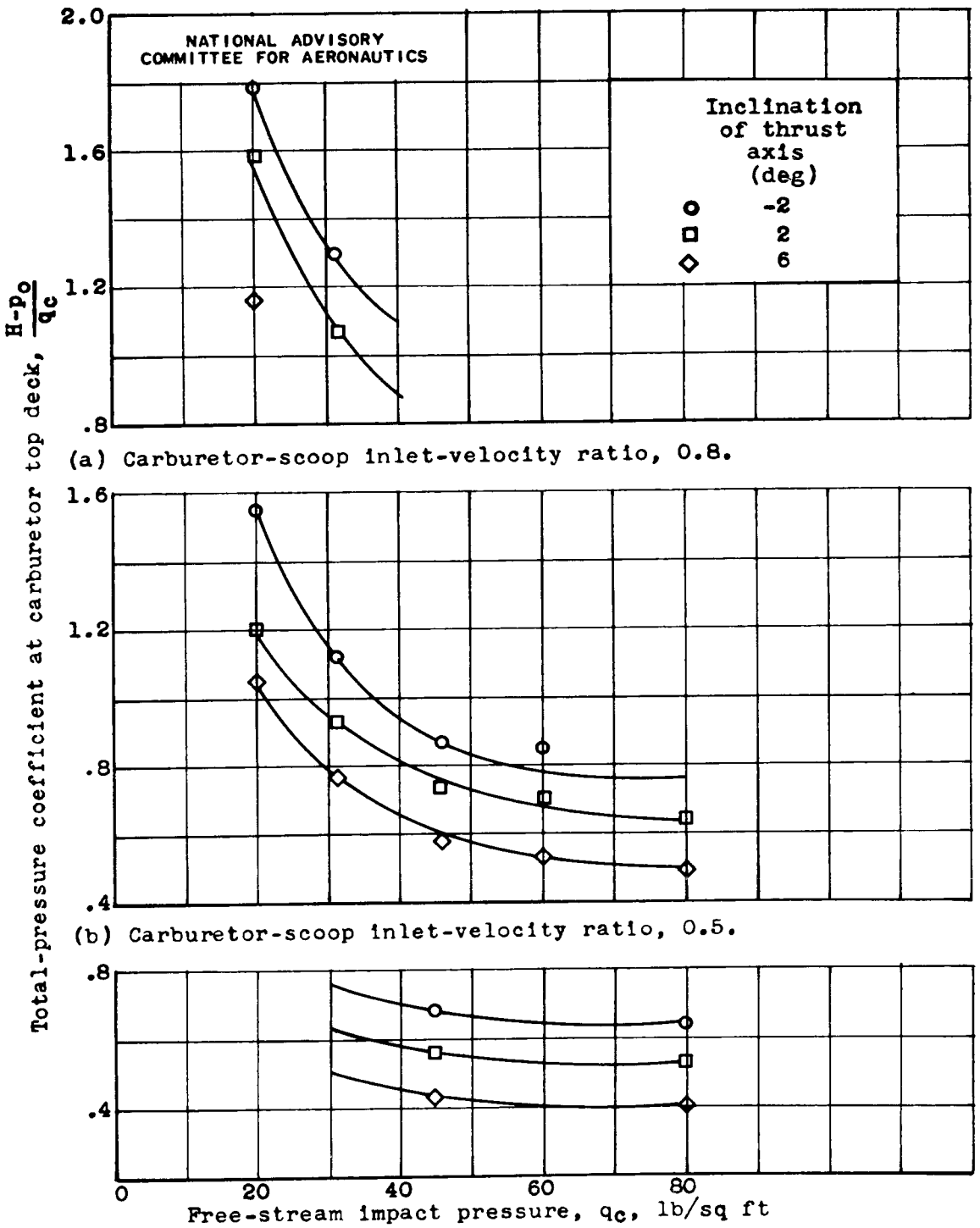

Figure 8. – Effect of free-stream impact pressure on total-pressure recovery at carburetor top deck of single-engine torpedo-bomber-type airplane for various inlet-velocity ratios and inclinations of thrust axis.

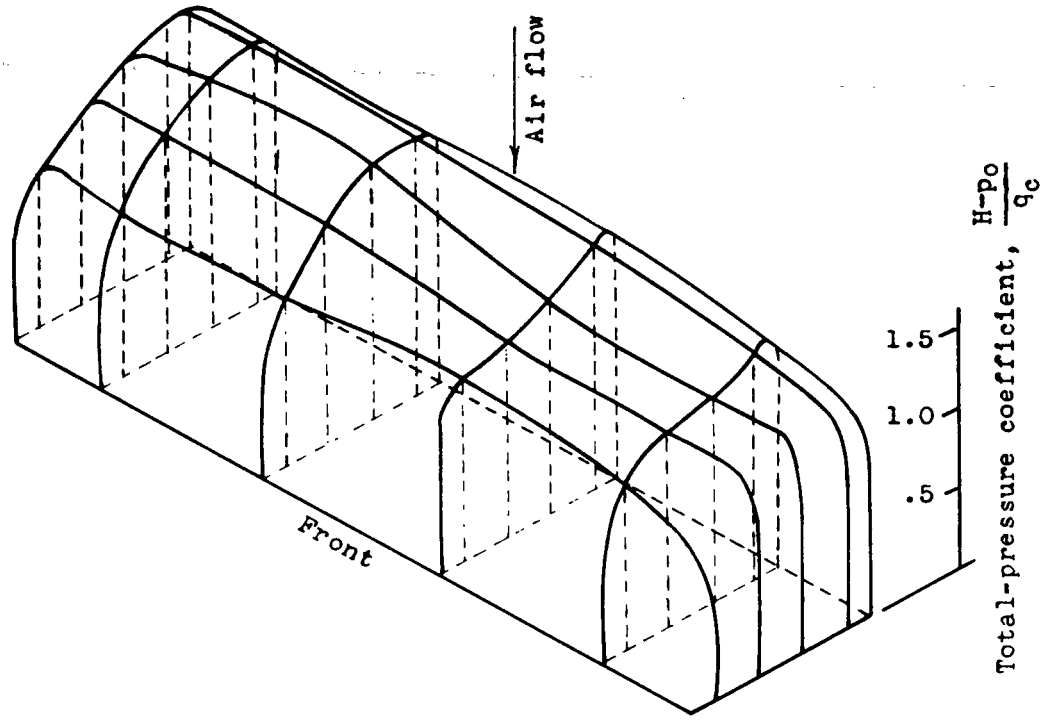

(a) Charge-air flow, 16,050 pounds per hour; free-stream impact pressure, q_c, 32 pounds per square foot; inclination of thrust axis, 6°; inlet-velocity ratio, 0.76.

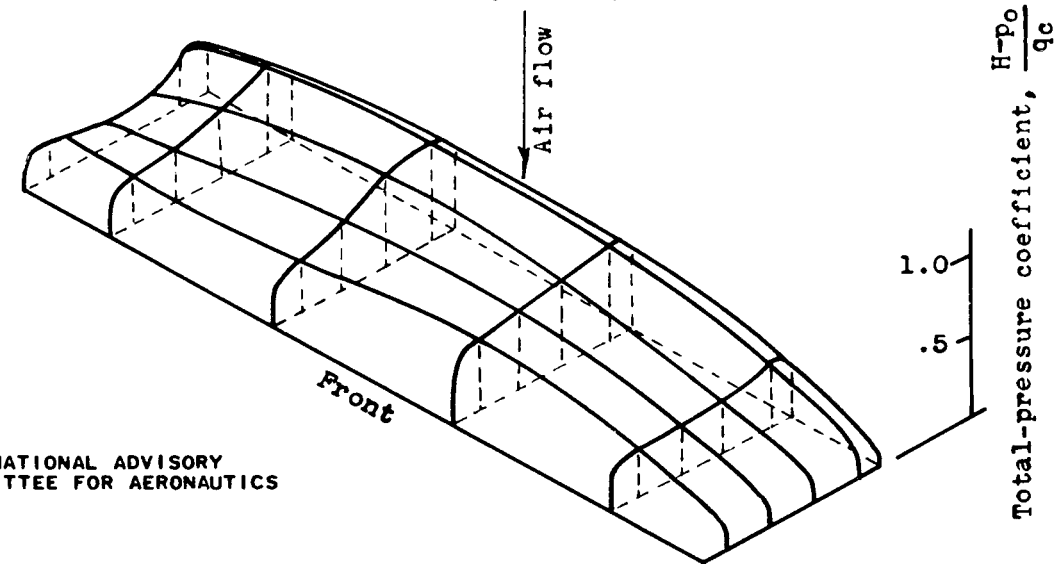

(b) Charge-air flow, 9460 pounds per hour; free-stream impact pressure, q_c, 92 pounds per square foot; inclination of thrust axis, 2°; inlet-velocity ratio, 0.26.

Figure 9. – Typical pressure distribution at carburetor top deck of single-engine torpedo-bomber-type airplane.

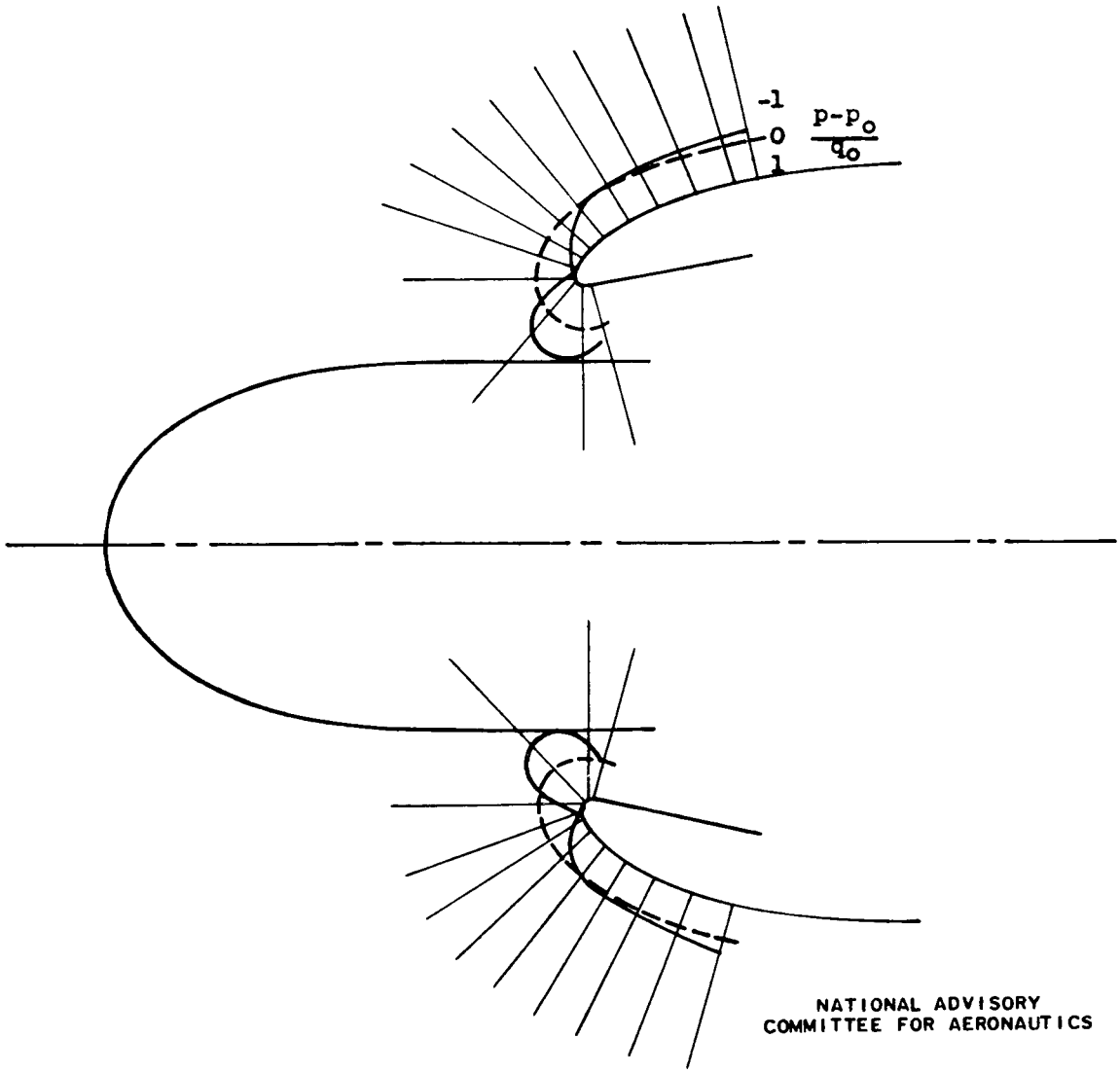

(a) Inclination of thrust axis, -2°; free-stream impact pressure, 78.5 pounds per square foot; brake horsepower, 1960.

Figure 10. - Cowl-lip static-pressure survey for single-engine torpedo-bomber-type airplane. Pressure altitude, 5000 feet; engine speed, 2650 rpm; cowl-flap deflection, 10°.

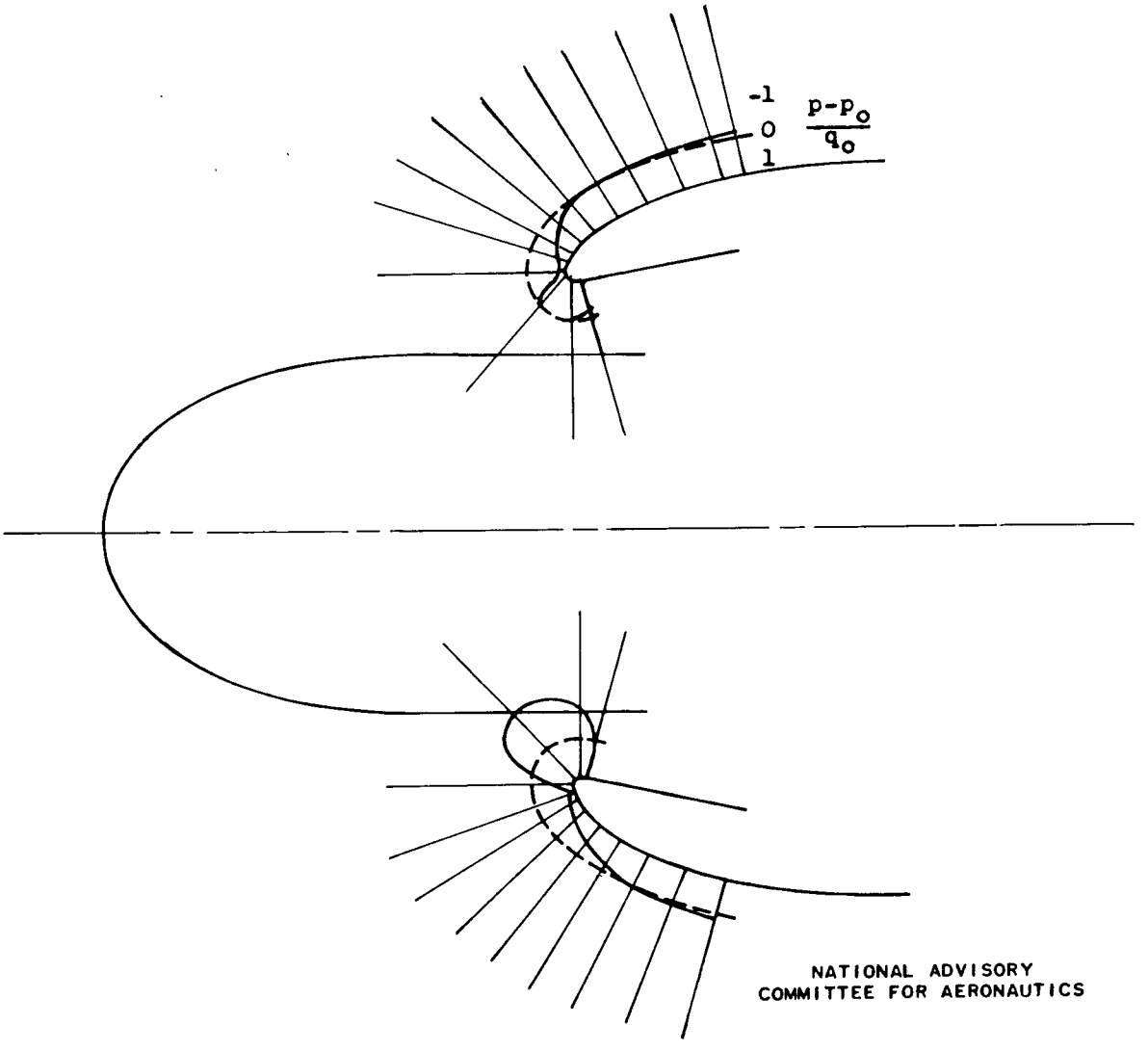

(b) Inclination of thrust axis, 2°; free-stream impact pressure, 79.0 pounds per square foot; brake horsepower, 1975.

Figure 10. – Continued. Cowl-lip-static-pressure survey for single-engine torpedo-bomber-type airplane. Pressure altitude, 5000 feet; engine speed, 2650 rpm; cowl-flap deflection, 10°.

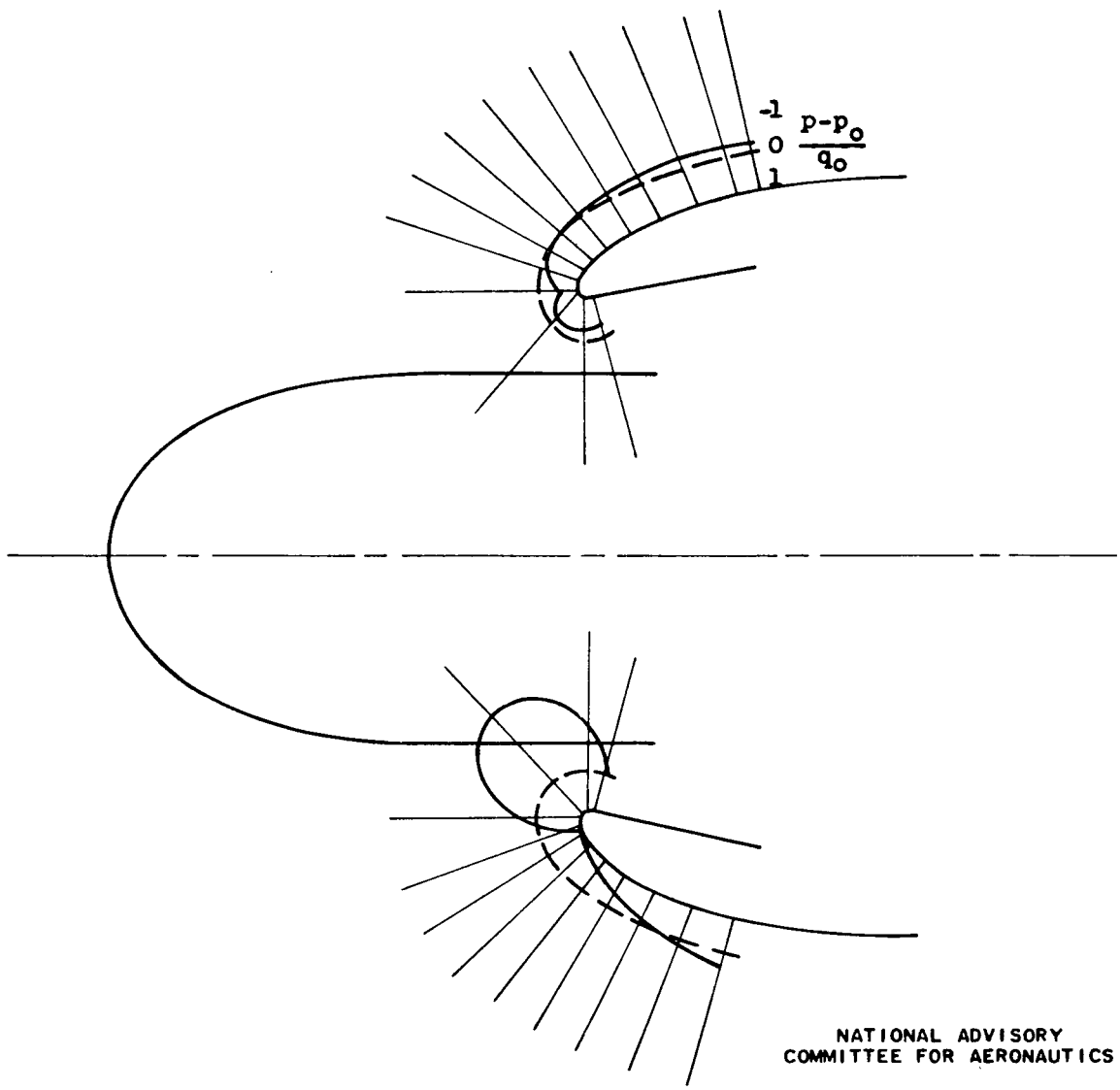

(c) Inclination of thrust axis, 6°; free-stream impact pressure, 78.5 pounds per square foot; brake horsepower, 1930.

Figure 10. - Concluded. Cowl-lip static-pressure survey for single-engine torpedo-bomber-type airplane. Pressure altitude, 5000 feet; engine speed, 2650 rpm; cowl-flap deflection, 10°.

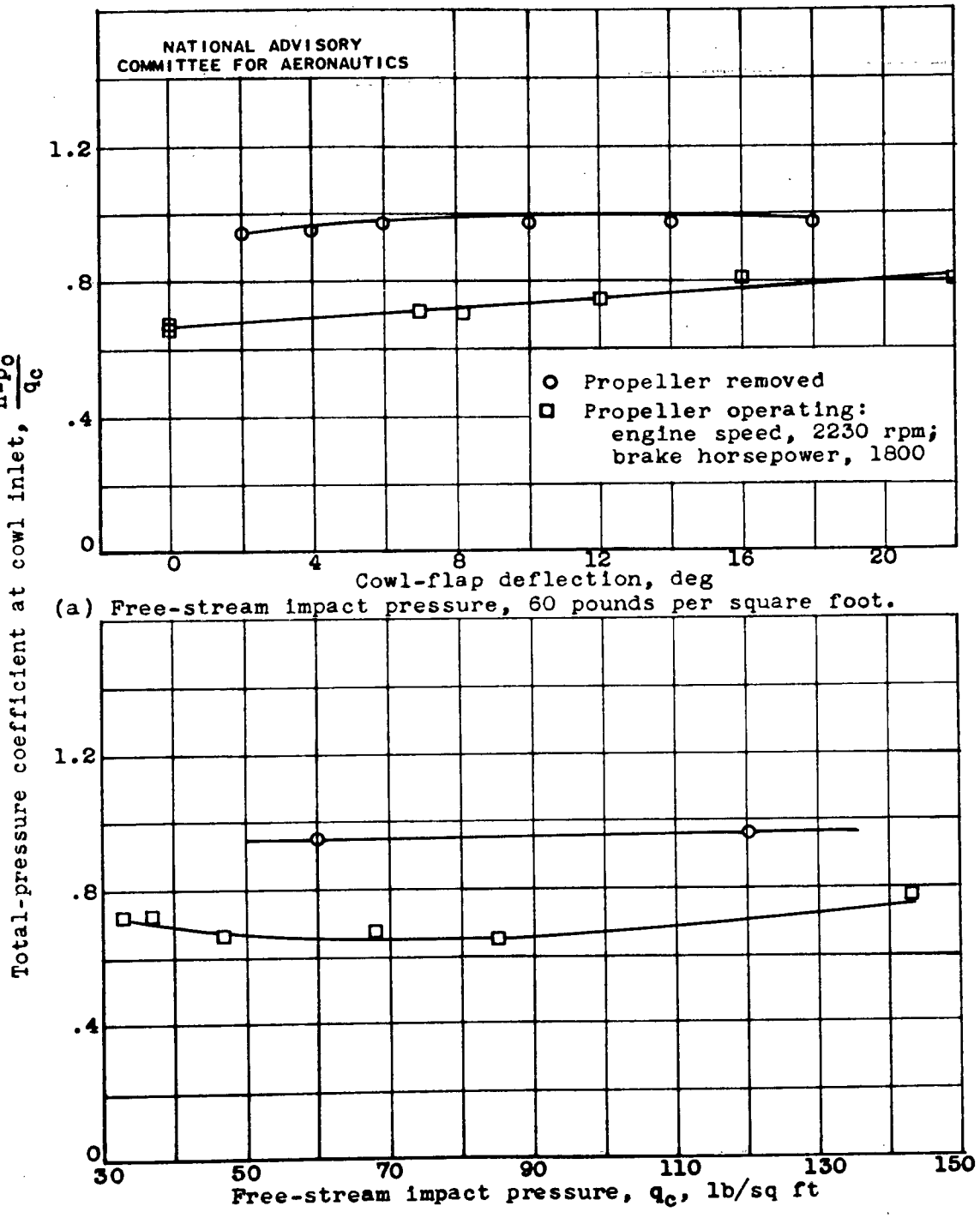

Figure 11. - Effect of cowl-flap deflection and free-stream impact pressure on total-pressure recovery at cowling inlet of single-engine torpedo-bomber-type airplane. Pressure altitude, 15,000 feet; inclination of thrust axis, 0°.

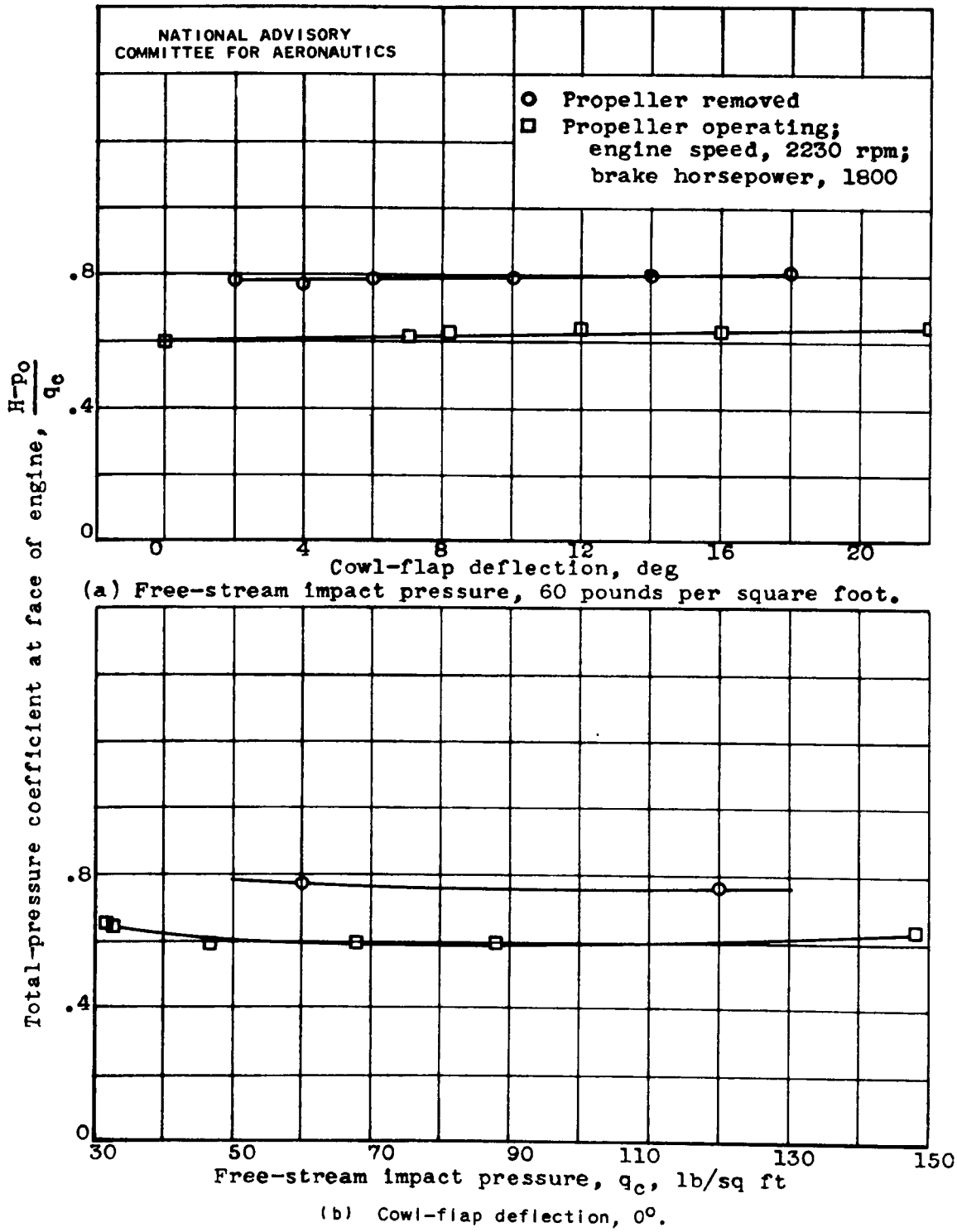

Figure 12. - Effect of cowl-flap deflection and free-stream impact pressure on total-pressure recovery at face of engine of torpedo-bomber-type airplane. Pressure altitude, 15,000 feet; inclination of thrust axis, 0°.

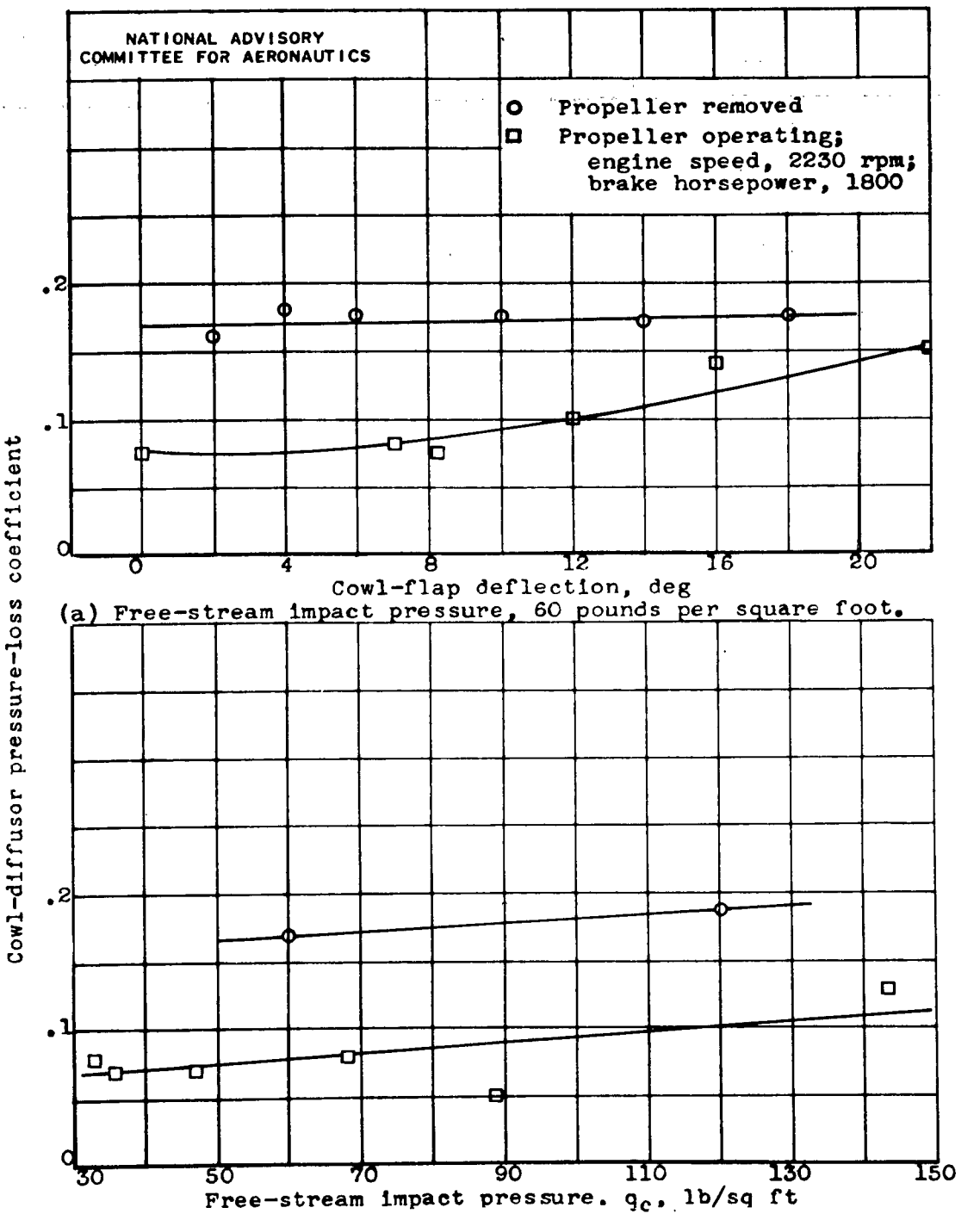

Figure 13. - Effect of cowl-flap deflection and free-stream impact pressure on cowl-diffuser pressure loss of single-engine torpedo-bomber-type airplane. Pressure altitude, 15,000 feet; inclination of thrust axis, 0°.

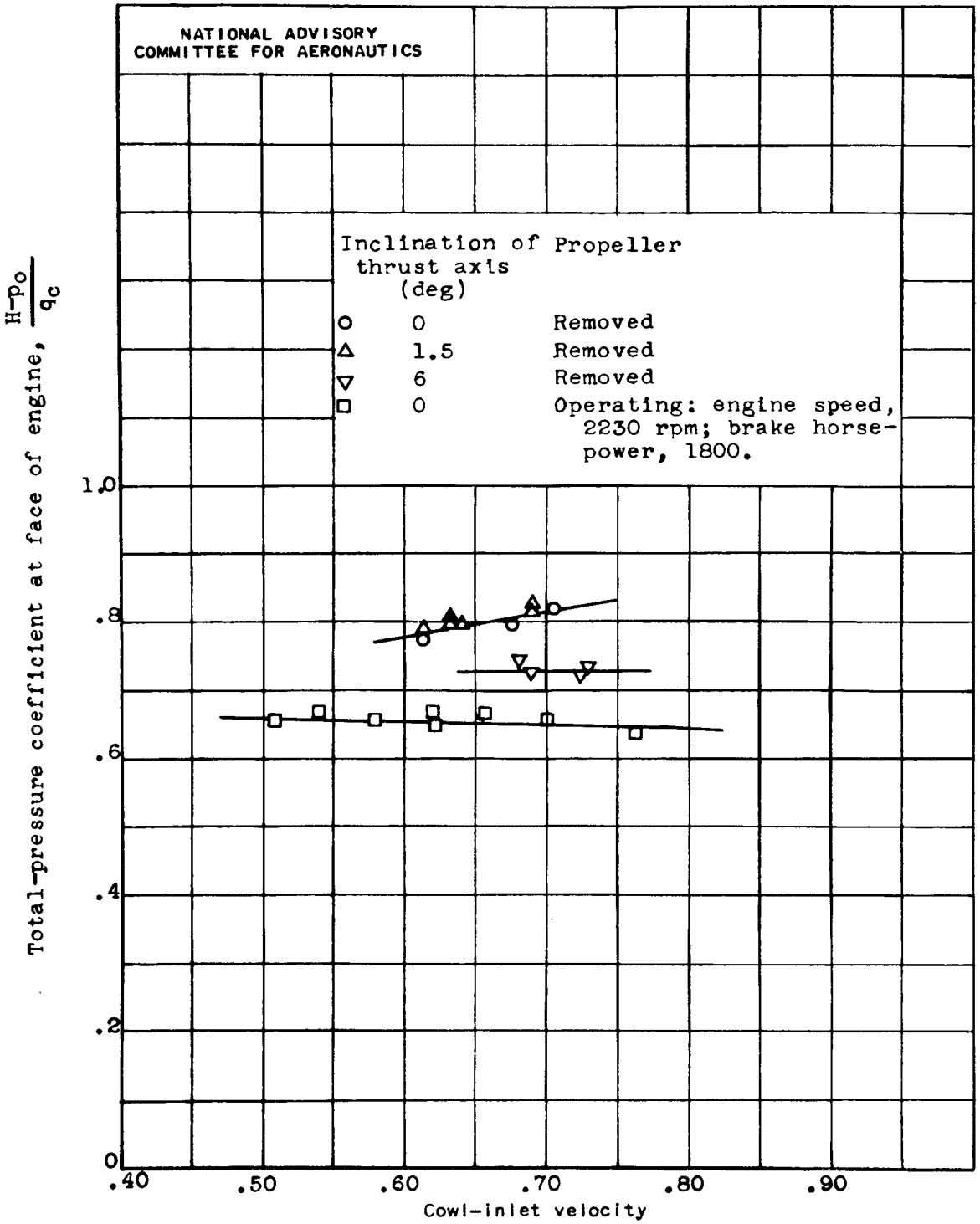

Figure 14. - Effect of cowl-inlet velocity ratio on total-pressure recovery at face of engine of torpedo-bomber-type airplane. Pressure altitude, 15,000 feet.

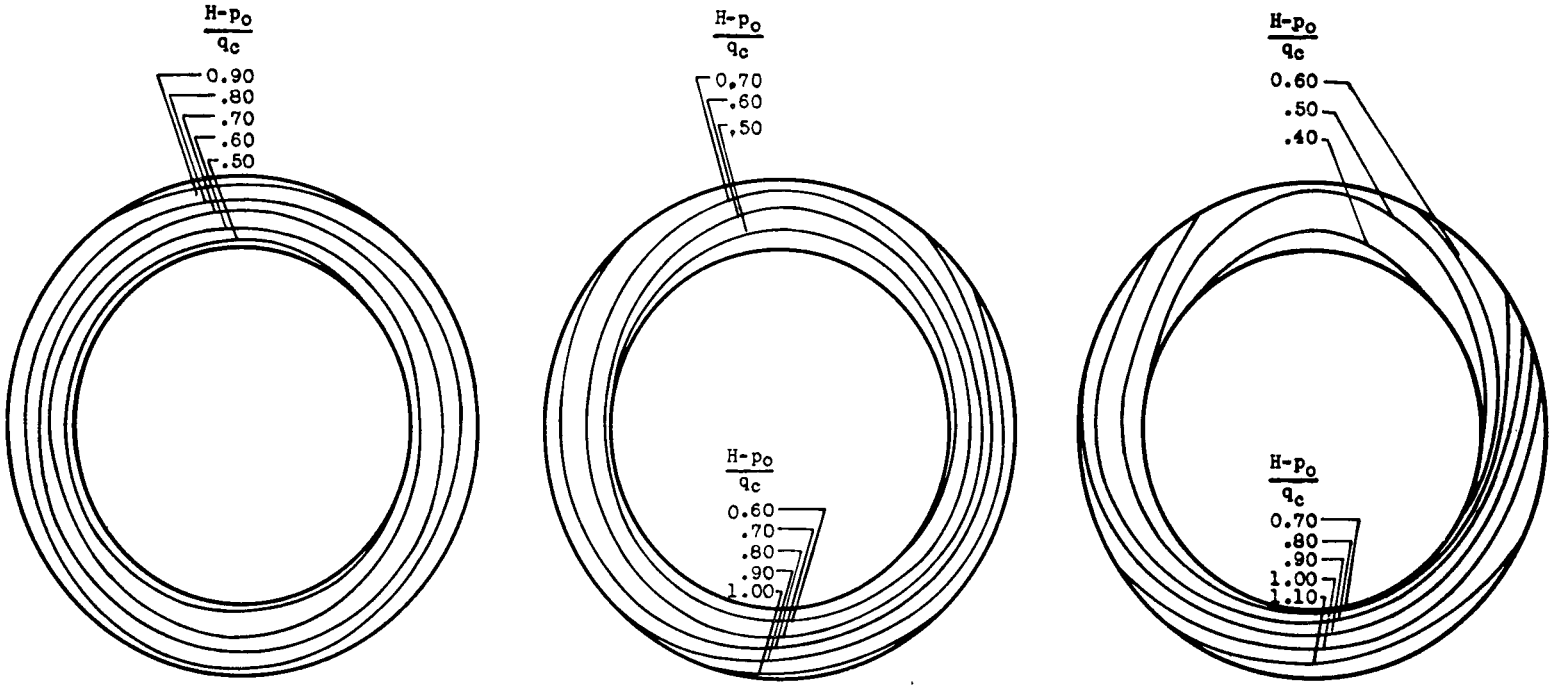

(a) Inclination of thrust axis. -2°. (b) Inclination of thrust axis. 2°. (c) Inclination of thrust axis. 6°.

Figure 15. - Total-pressure distribution at cowling inlet of single-engine torpedo-bomber-type airplane with propeller operating. Brake horsepower, 1530; engine speed, 2450 rpm; free-stream impact pressure, 46 pounds per square foot; inlet-velocity ratio, 0.76; pressure altitude, 5000 feet.

NATIONAL ADVISORY
COMMITTEE FOR AERONAUTICS

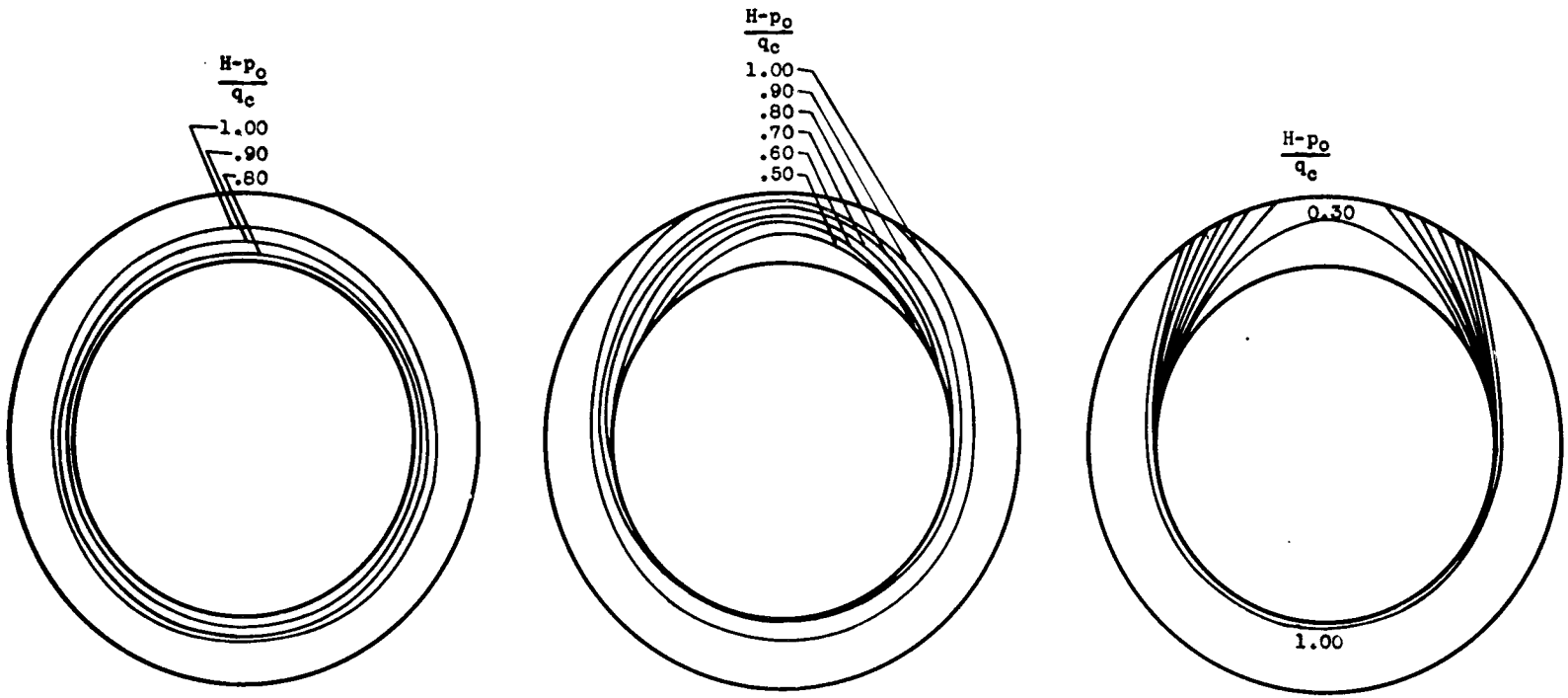

(a) Inclination of thrust axis, 0°. (b) Inclination of thrust axis, 1.5°. (c) Inclination of thrust axis, 6°.

Figure 16. - Total pressure distribution at cowling inlet of single-engine torpedo-type-bomber airplane with propeller removed. Free-stream impact pressure, 60 pounds per square foot; inlet-velocity ratio, 0.63; pressure altitude, 15,000 feet.

NATIONAL ADVISORY
COMMITTEE FOR AERONAUTICS.

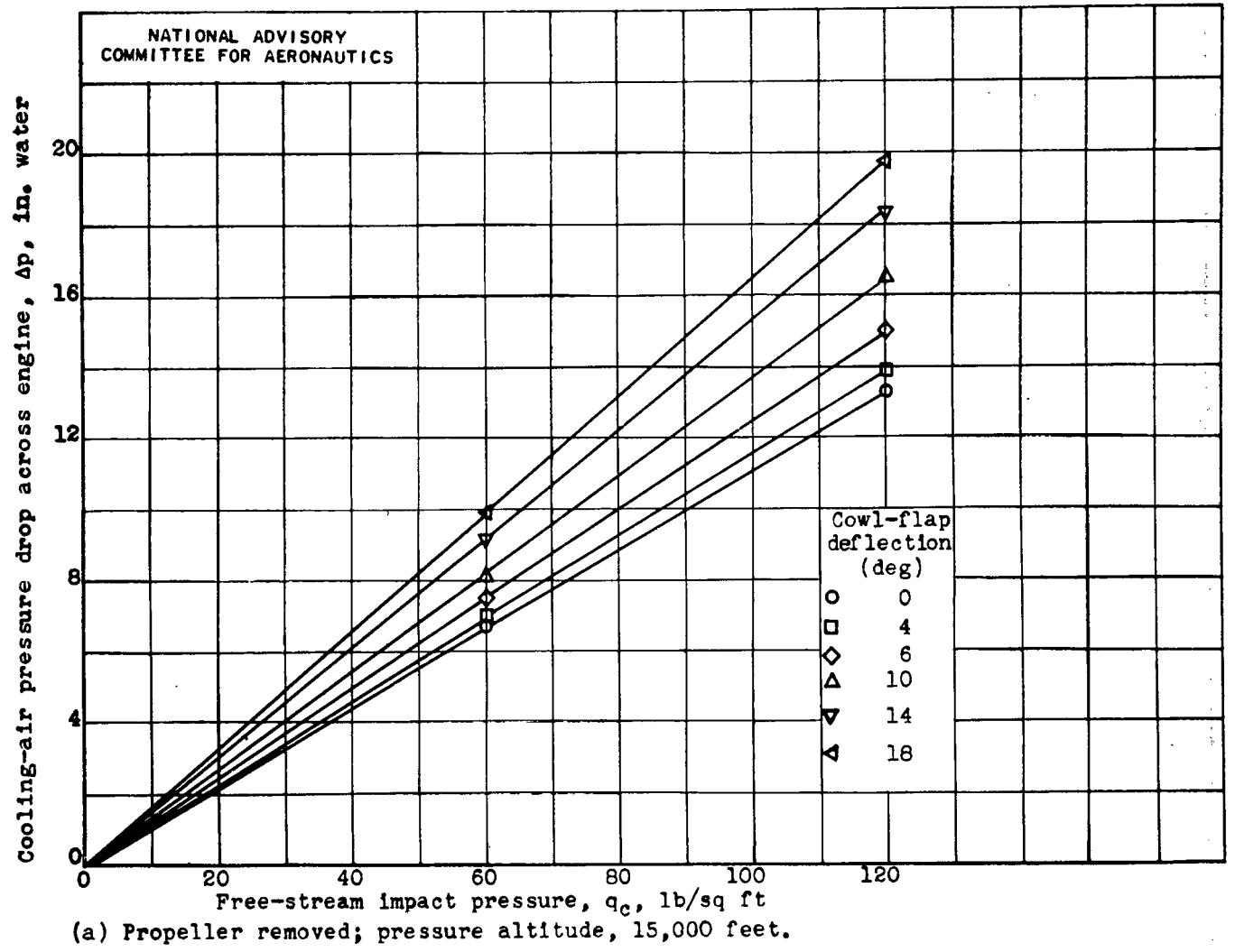

(a) Propeller removed; pressure altitude, 15,000 feet.

Figure 17. - Effect of free-stream impact pressure on cooling-air pressure drop across engine of torpedo-bomber-type airplane at various cowl-flap deflections. Inclination of thrust axis, 0°.

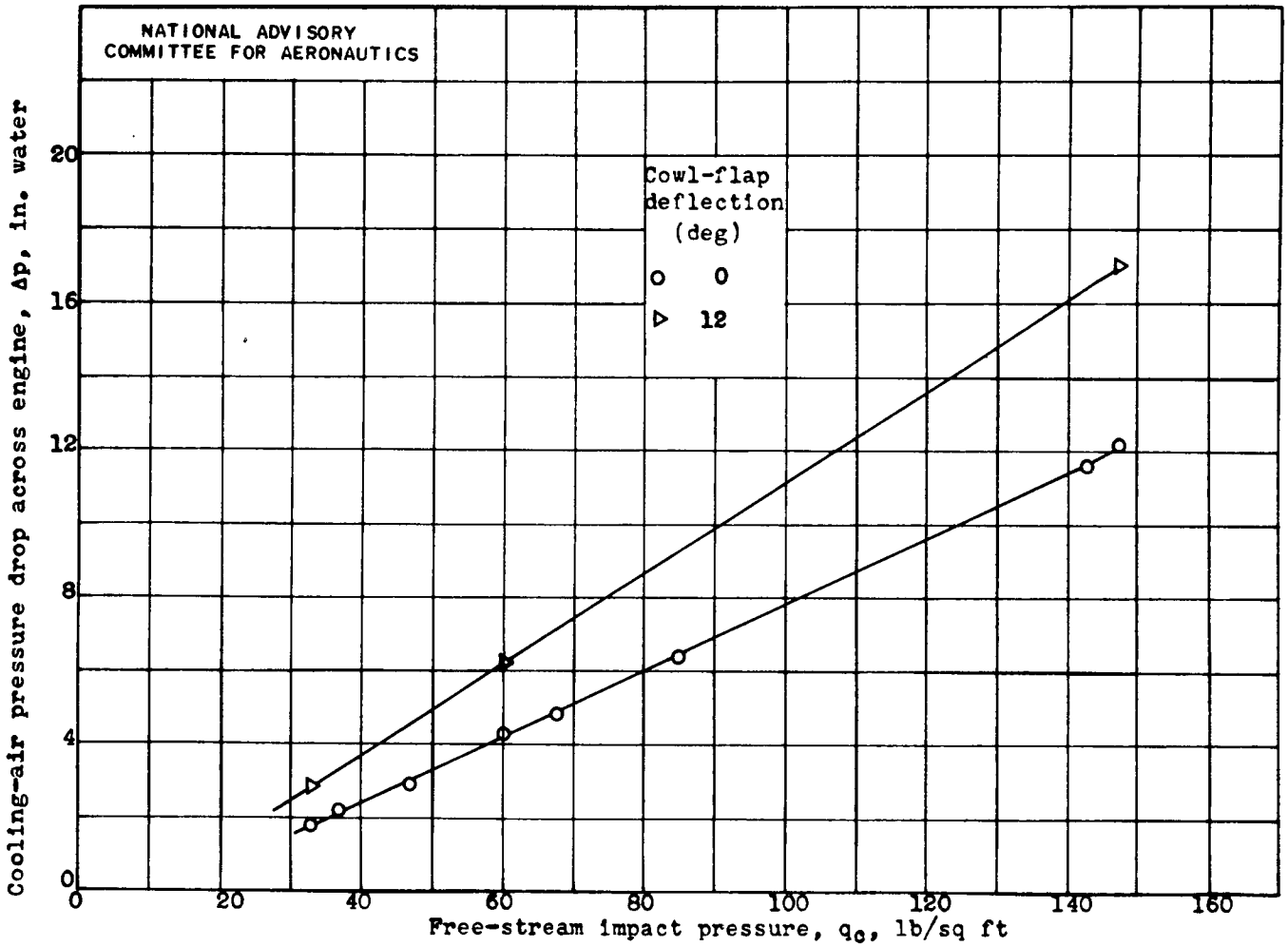

(b) Propeller operating; brake horsepower, 1800; engine speed, 2230 rpm; pressure altitude, 15,000 feet.

Figure 17.- Continued. Effect of free-stream impact pressure on cooling-air pressure drop across engine of torpedo-bomber-type airplane at various cowl-flap deflections. Inclination of thrust axis, 0°.

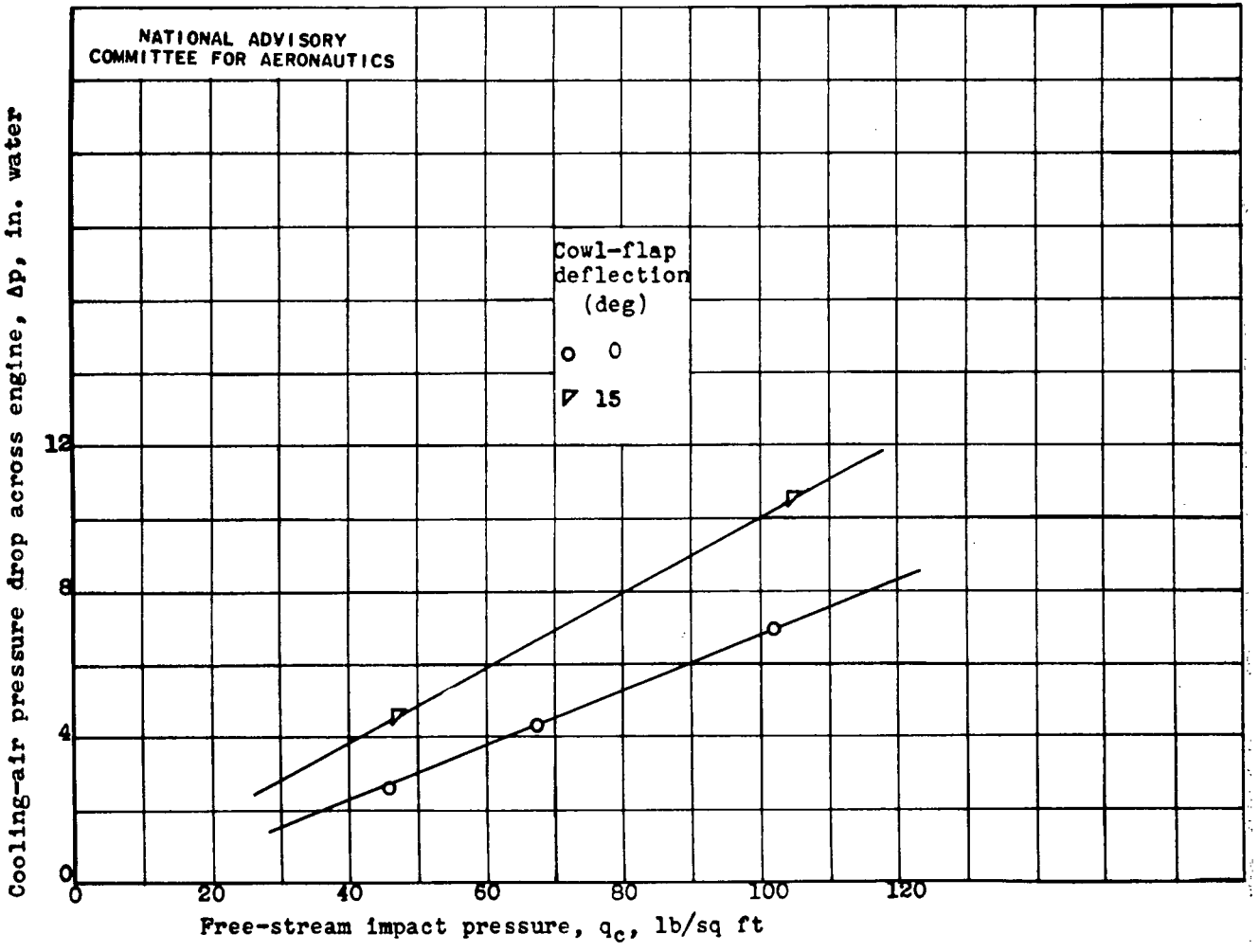

(c) Propeller operating; brake horsepower, 1520; engine speed, 2230 rpm; pressure altitude, 30,000 feet.

Figure 17. - Concluded. Effect of free-stream impact pressure on cooling-air pressure drop across engine of torpedo-bomber-type airplane at various cowl-flap deflections. Inclination of thrust axis, 0°.

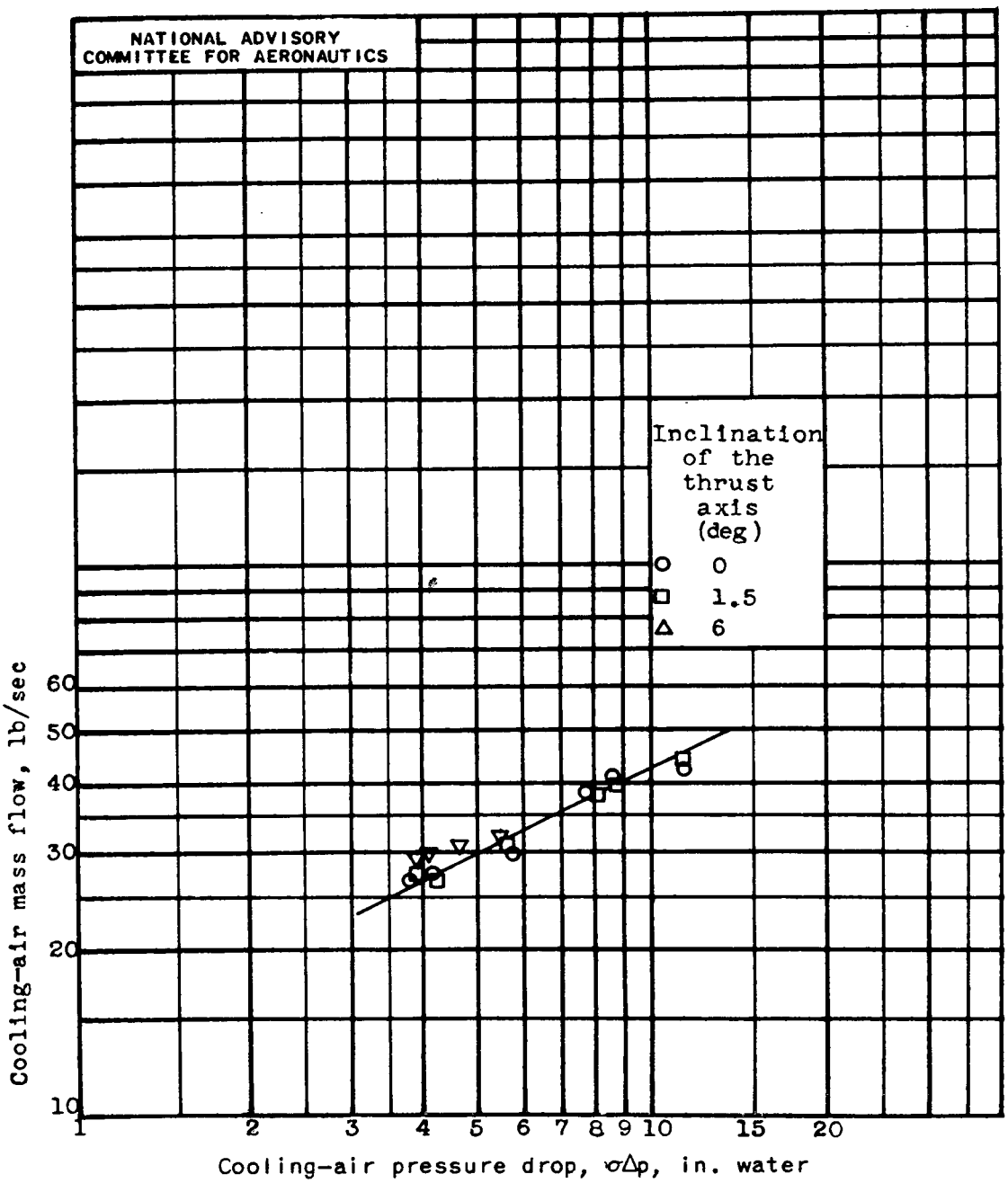

Figure 18. – Relation of cooling-air pressure drop to cooling-air mass flow for tests of single-engine torpedo-bomber-type airplane with propeller removed. Pressure altitude, 15,000 feet.

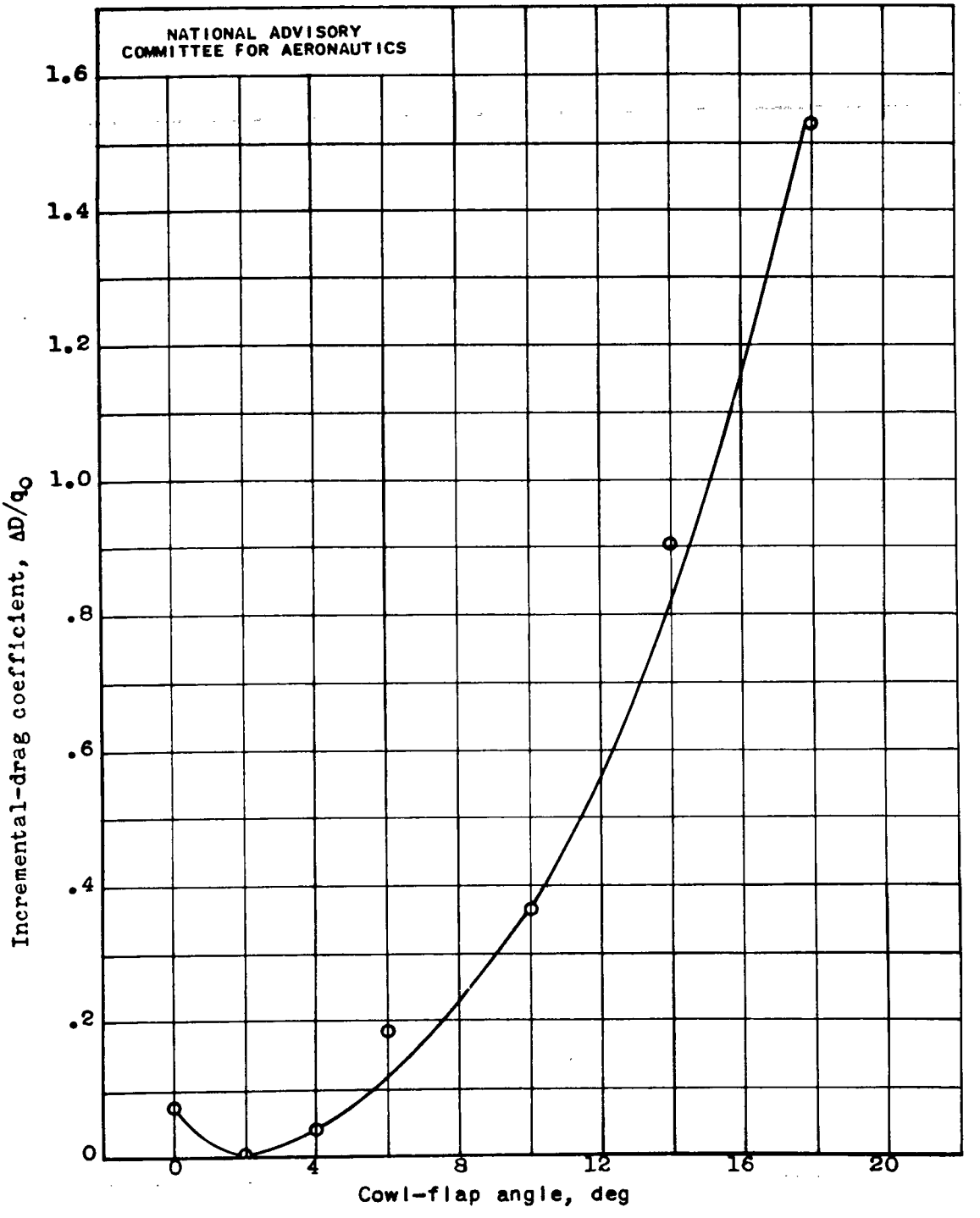

Figure 19. - Variation in incremental-drag coefficient with cowl-flap angle for single-engine torpedo-bomber-type airplane. Propeller removed; pressure altitude, 15,000 feet; inclination of thrust axis, 0°.

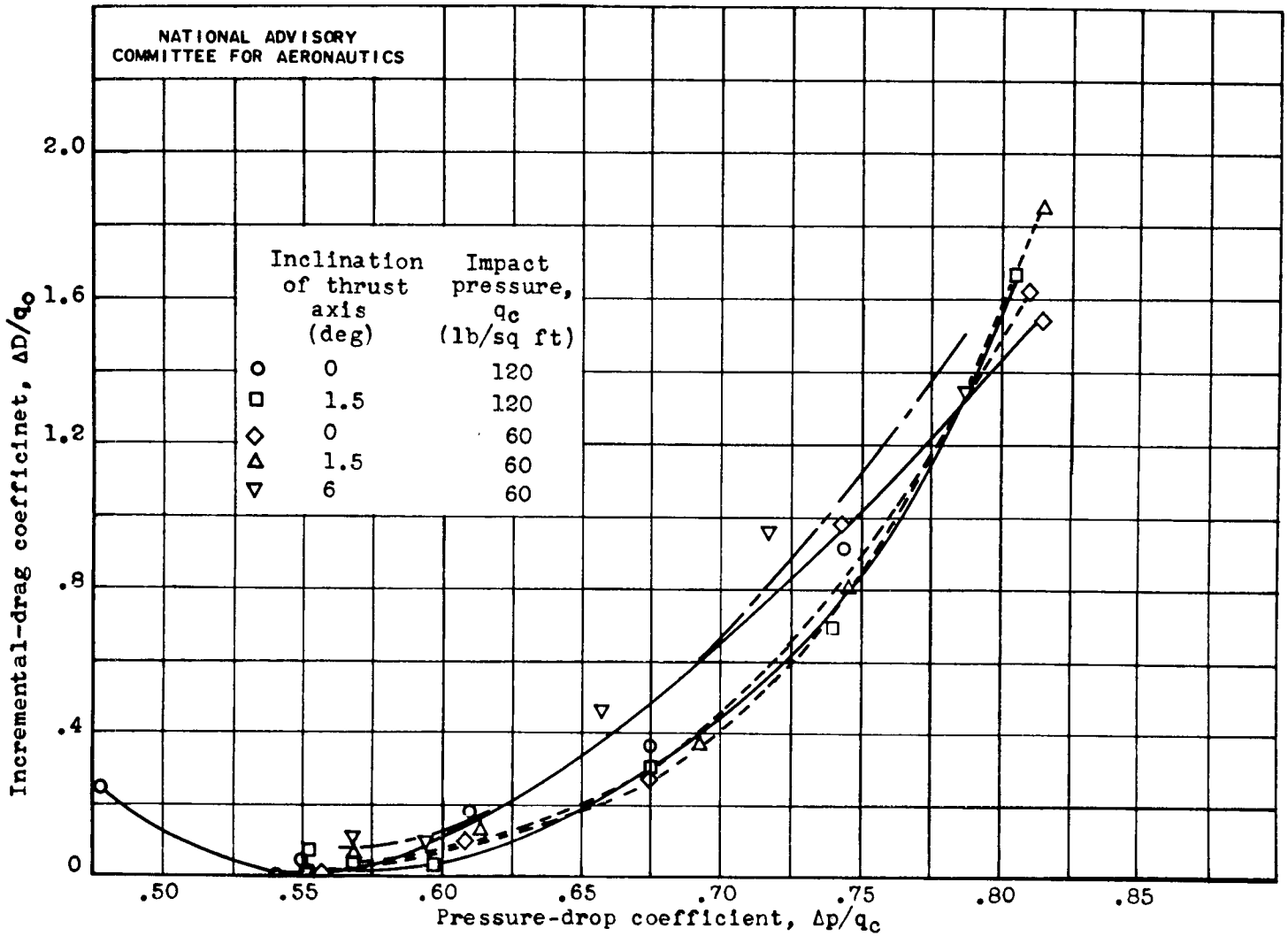

Figure 20. - Variation of incremental-drag coefficient with pressure-drop coefficient across engine of torpedo-bomber-type airplane.